



Published in final edited form as:

European J Org Chem. 2020 March 15; 2020(10): 1259–1273. doi:10.1002/ejoc.201901229.

Visible-Light-Induced Dearomatizations

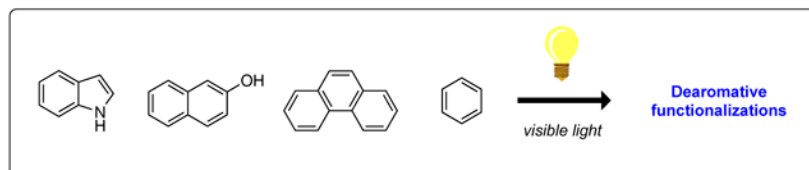
Mikiko Okumura^a, David Sarlah^a

^[a]Roger Adams Laboratory, Department of Chemistry, University of Illinois, Urbana, Illinois 61801, USA

Abstract

The dearomatization of aromatic compounds is an important synthetic strategy used in accessing complex three-dimensional structures from simple aromatic precursors. This minireview aims to provide an overview of recent advancements in this area, with a specific focus on visible-light-mediated dearomative transformations. Compared to the conventional high-energy ultraviolet (UV) light-promoted processes, not only these new approaches offer milder reaction conditions to accommodate wider variety of substrates with sensitive functionalities, but also enable the use of photocatalysts and other promoters, significantly expanding the reaction space. Application of these transformations to the synthesis of bioactive compounds are also discussed.

Graphical Abstract



This minireview covers a recent progress made in dearomative transformation methods which utilize visible light as a means to facilitate dearomatization. Unique and complex alicyclic scaffolds prepared from a wide variety of simple arenes will be discussed.

Keywords

dearomatization; visible light; arene; functionalization; photochemistry

1. Introduction

Aromatic compounds represent one of the most abundant classes of organic molecules, characterized by unique chemical properties and transformations.^[1] In particular, dearomatization processes play an important role in converting readily available arenes into more valuable alicyclic hydrocarbon frameworks.^[2] Notable examples include dissolving metal (Birch) reduction,^[3] transition-metal catalyzed hydrogenation,^[4] oxidative phenol dearomatization,^[5] and transition-metal-mediated dearomative functionalization,^[6] all of

which are considered to generate rapid complexity, ultimately offering facile access to important scaffolds with functional and stereochemical diversity.

Among dearomatizations, the application of photochemistry has a long and rich history. While aromatic compounds are generally considered to be inert and challenging to dearomatize due to their resonance stabilization energies, high-energy ultraviolet (UV) light has been successfully utilized to photoactivate the arenes, generating reactive intermediates that could be further converted to stable dearomatized carbocycles.^[7] Along these lines, arene-alkene photocycloadditions are the most well-explored processes in this field, providing *ortho*-, *meta*-, or *para*-periselectivity, depending on the substrate employed.^[8] Despite the development of many effective transformations, the major disadvantages of these dearomative processes come from the poor product selectivity and functional group compatibility due to the harsh, high-energy UV light conditions required. Nonetheless, these transformations have provided access to unique alicyclic structures that are otherwise difficult, or even impossible to synthesize by other means.

On the other hand, the use of visible light as a mild source of energy for a chemoselective generation of reactive radical intermediates has recently emerged as a powerful synthetic tool, represented by advancements in the field of photoredox catalysis.^[9] Moreover, a variety of visible-light-absorbing molecules, both organic and inorganic, have been identified to effectively activate aromatic substrates via single-electron-transfer (SET) and/or energy transfer (ET) processes upon photoexcitation with visible light, resulting in a range of bond-forming and cleavage processes with minimal side reactions. It comes with no surprise that such trends have significantly influenced the pursuits for effective dearomative transformations of readily available arenes. Thus, visible-light-mediated transformations have become a key strategy in modern organic chemistry for developing milder and more enabling dearomative processes, and significant progress has been made in terms of the type of the transformations as well as the scope of arenes that are capable of engaging in such processes. To this end, the objective of this review is to highlight recent literature reports involving visible-light-mediated dearomative functionalization protocols. Focus is given primarily to processes that utilize a combination of visible-light-promoted chemical reactions and dearomative functionalizations, whereby a light-mediated chemical phenomenon promotes the subsequent dearomative transformations. Processes that use light sources other than visible light, or dearomative transformations that are followed by re-aromatization are not covered here, and the readers are referred to several excellent reviews on these topics.^[7,8] Since most of the arenes themselves do not directly absorb visible light, this review is organized by means of arene activation mode: 1) assisted photoactivation of arenes, 2) arenophile-mediated dearomatization, and 3) dearomatization via photochemically generated reactive radical intermediates.

2. Assisted photoactivation of arenes

2.1. Dearomatization of indoles and naphthols through visible-light photoredox catalysis

In 2016, Zhu and co-workers reported a method for the synthesis of heterocycle fused indolone **1** through a visible-light-mediated aerobic dearomatization of indole derivatives bearing a nucleophilic side chain at position N-1 (Scheme 1A).^[10] The proposed reaction

mechanism of this process begins with a photoinduced single electron oxidation of indole **2** by $[\text{Ru}(\text{bpy})_3^{2+}]^*$ to indolyl radical cation **3**, and the oxidation of resulting $[\text{Ru}^+]$ complex by molecular oxygen back to $[\text{Ru}(\text{bpy})_3^{2+}]$, providing a superoxide radical anion (Scheme 1B). This highly reactive species then reacts with indolyl radical **3** to generate intermediate **4** or **5**, which then undergoes intramolecular nucleophilic attack by the alcohol side chain, giving the corresponding peroxide **6**; subsequent base-mediated Kornblum-DeLaMare rearrangement affords oxazolo[3,2-*a*]indolone **7**. The authors optimized the reaction parameters and found that utilizing cesium acetate as a base additive in acetonitrile under an oxygen atmosphere gave the best results for a variety of substituted indole derivatives (Scheme 1C). Similarly, spiro[furan-2,2'-indolin]one and spiro[pyran-2,2'-indolin]one could be synthesized using the same protocol by tethering the alcohol moiety at the C-2 position of the unprotected indole (Scheme 2).

In 2019, Zheng, Zhang, You, and co-workers reported a dearomative functionalization protocol of indole derivatives based on visible-light-promoted dearomatization and [2+2] cycloaddition (Scheme 3A).^[11] From experimental and computational analyses, the initial indole dearomatization was thought to proceed via an energy transfer mechanism from the excited photoredox catalyst to the ground state indole **11** (Scheme 3B). This process forms a triplet diradical intermediate **12**, which then undergoes intramolecular [2+2] cycloaddition with appended alkene functionality, providing highly strained cyclobutane-fused angular tetracyclic spiroindoline **13**. With $[\text{Ir}(\text{dFCF}_3\text{ppy})_2(\text{dtbbpy})]\text{PF}_6$ (**9**) as a catalyst under blue LED irradiation, indoles with different linkages on the substituent at C-3 position gave the corresponding tetracyclic spiroindolines (Scheme 3C). Notably, the electronic nature of the C-2 substituent (R^1 group) had a significant effect on the reaction outcome, with electron-withdrawing groups generally enhancing the transformation. While electron-donating group on the indole N-1 position (R^2 group) diminished the yield, electron-withdrawing groups such as acetate and trifluoroacetate groups greatly promoted the reaction. As illustrated in Scheme 4, this method could also generate tetracyclic spiroindolines with three contiguous all-carbon quaternary stereogenic centers in a single step, when indoles bearing substituted olefins were employed.

Naphthols are also viable substrates for the direct activation with photoredox catalysts. In 2018, You and co-workers reported an intermolecular oxidative dearomatization of 2-naphthols **14** with *N*-hydroxycarbamates (Scheme 5A).^[12] The use of $[\text{Acr-Mes}]\text{ClO}_4$ (**15**) as a photoredox catalyst under air was essential in achieving this transformation, which led to a selective photoactivation of naphthol **14** to radical cation intermediate **17**, followed by nucleophilic capture of the resulting radical cation **17** by the carbamate with exclusive C–O bond-forming selectivity (Scheme 5B). Then, the radical intermediate **18** underwent a single-electron oxidation by the superoxide anion, formed as a result of acridinium catalyst regeneration, and subsequent deprotonation afforded naphthalenone **16**. This dearomative process tolerated a variety of functional groups, including halogens, alkenes and electron-rich arene functionality (Scheme 5C).

An elegant dearomative cascade promoted by photocatalysis with 1-naphthol-derived arenes was reported by Glorious and co-workers, which afforded two different polycyclic scaffolds (Scheme 6A).^[13] Accordingly, the choice of photocatalyst as well as solvent had profound

effects on the reaction outcomes. While catalyst **22** in methanol predominantly formed styrene **20**, catalyst **9** in 1,4-dioxane promoted the formation of product **21**. Based on a series of mechanistic studies, the authors proposed a reaction mechanism involving energy transfer from excited Ir-photocatalyst **22** or **9** to the substrates rather than a photoinduced SET process (Scheme 6B). The resulting triplet naphthol **24*** underwent an intramolecular dearomative [2+2] cycloaddition with appendant alkene to afford styrene **25**. The π -system of the styrene **25** could engage in another energy transfer event to form triplet styrene **25***, and trigger a vinylcyclobutane rearrangement to afford benzocyclobutene **28** via diradical intermediates **26** and **27**. Computational studies suggested this second energy transfer was more favorable using Ir-catalyst **9** as a photosensitizer, thus enabling a divergent synthesis of two different polycyclic scaffolds from a single arene. As for the substrate generality, electron-withdrawing group at C-2 position of naphthol was necessary to ensure the reactivity, both aliphatic ketones and methyl ester promoted the reaction smoothly (Scheme 7). Finally, a diverse range of substituents on both rings of the naphthol system was well tolerated.

2.2. Photoactivation of arene–chiral Lewis acid complex

Visible-light-promoted processes that rely on the use of Lewis acids to induce a bathochromic absorption shift are becoming a popular approach in achieving selectivity of photochemical transformations. Such a concept was also applied for the development of several enantioselective dearomatizations. Bach and co-workers demonstrated a visible-light-induced enantioselective *ortho*-photocycloaddition of olefins to phenanthrene-9-carboxaldehyde derivatives with chiral oxazaborolidine Lewis acid (**29**) as a catalyst (Scheme 8).^[14] Interestingly, the arene scope of this dearomative cycloaddition with 2,3-dimethyl-2-butene revealed the importance of C-3 and C-6 phenanthrene substituents on enantioinduction, as substitution at C-2 and C-5 position lead to a significant decrease in the enantioselectivity. In addition to acyclic substrates, symmetrical cyclic olefins also proved to be viable reactants, with cyclopentene giving higher enantioselectivity as well as diastereoselectivity than cyclohexene.

Catalytic asymmetric dearomatization through visible-light-promoted [2+2] photocycloaddition was also reported by Baik, Meggers, and co-workers using Lewis acid activation. In this case, the authors used visible-light-activatable chiral Lewis acid catalyst **-RhS** with benzofurans and a benzothiophene bearing *N*-acylpyrazole moiety **31** (Scheme 9).^[15] Using styrenes as the olefin coupling partners, cycloadducts of type **32** were isolated, upon methanolysis, as single diastereomers in good yields and in high enantioselectivity. The ratio of constitutional isomers was highly dependent on the nature of styrene starting material.

The mechanism of this catalytic dearomatization is proposed to begin with association of *N*-acylpyrazole **31** and chiral rhodium catalyst **-RhS** to form complex **33**, which is promoted to its singlet excited state **34** after irradiation with blue LED light (Scheme 10). Intersystem crossing forms triplet reactant **35**, and the addition of the resulting radical species to styrene gives 1,4-biradical intermediate **36**. This intermediate undergoes radical recombination,

affording the cycloadduct **37**. Finally, the regeneration of the catalyst, as well as the release of the product **38** is accomplished by decomplexation.

2.3. Photoactivation of electron donor–acceptor (EDA) complex

Although limited in number, visible-light-induced dearomatization processes that rely on a formation of electron donor-acceptor (EDA) and/or intermolecular charge transfer complexes between arenes and the reactants have also been documented. The EDA complexes utilized in these reactions exhibit a characteristic bathochromic shift in their absorption spectrum to the visible region, thus allowing the reactions to be carried out without the need of either external photocatalysts or other promoters.

In 2018, You and co-workers reported a cascade alkene trifluoromethylation with subsequent dearomatization of indole derivative **38** using Umemoto's reagent (**39**) as a trifluoromethyl source (Scheme 11A).^[16] Based on several mechanistic studies, a plausible mechanism of this transformation begins with the formation of transient EDA complex (**41**) between indole and Umemoto's reagent, followed by SET from donor to acceptor upon visible-light irradiation (Scheme 11B). Trifluoromethyl radical, generated from the transient excited species **42** via homolytic S–CF₃ bond cleavage, added into the alkene functionality on indole **43**, and subsequent radical–radical recombination afforded the product **45**. Functional groups at various positions of the indole were compatible with this dearomative protocol (Scheme 11C). With regard to the tethered olefin partner, only terminal monosubstituted alkene were examined in this report. Furthermore, a mixture of diastereoisomers was observed in all cases.

Dearomative perfluoroalkylation of 2-naphthols with fluoroalkyl iodides through a visible-light-induced intermolecular charge transfer process was realized by Wang, Xu, and co-workers (Scheme 12A).^[17] A radical chain propagation pathway was proposed for this transformation with calculated quantum yield of $\phi = 14$, where visible light irradiation of EDA complex **47**, formed between deprotonated 2-naphthol and fluoroalkyl iodide, underwent SET, generating perfluoroalkyl radical (Scheme 12B). The reaction was propagated through addition of the resulting perfluoroalkyl radical species to the deprotonated β -naphthol (**48**), followed by abstraction of iodide from fluoroalkyl iodide to regenerate perfluoroalkyl radical and furnish desired product **46**. A variety of functionalities at the C-1 and C-3 positions were tolerated, including more sensitive groups such as halides, alkenes, and alkynes; notably, fluoroalkyl iodides with various alkyl chain length promoted the reaction smoothly (Scheme 12C). Furthermore, one example for dearomative fluoroalkylation of substituted phenol **51** was reported under the same reaction conditions (**52**).

3. Arenophile-mediated dearomative strategies

A conceptually distinct approach toward dearomative functionalization of arenes was demonstrated by Sarlah and co-workers by means of *arenophiles*.^[18] First reported by Sheridan and co-workers in 1984, arenophiles such as *N*-methyl-1,2,4-triazoline-3,5-dione (MTAD, **53**)^[19] can react with simple arenes at low temperatures upon irradiation of visible light, undergoing *para*-cycloaddition (Scheme 13A).^[20] The resulting arene-arenophile

cycloadducts of type **54** require generation at cold temperatures, as retrocycloaddition proceeds above $-20\text{ }^{\circ}\text{C}$. Although the mechanism of this process is not yet fully established, several studies indicate either or both electron transfer and charge transfer process occur between arenes and the photoactivated MTAD (Scheme 13B).^[21] Based on this unique arenophile photoreactivity, Sarlah and co-workers developed two general dearomative strategies: 1) olefin-like dearomative functionalization and 2) transition-metal-catalyzed dearomative aminofunctionalization. In this subsection, both approaches will be discussed, as well as their synthetic applications.

3.1. Arenophile-mediated olefin-like dearomative functionalization

Having recognized the potential for arene-MTAD cycloadduct serving as a formal surrogate of an arene with an isolated olefin, Sarlah and co-workers first developed a protocol for arenophile-mediated dearomative dihydroxylation (Scheme 14).^[22] In this process, mononuclear arene-MTAD cycloadducts were directly subjected to OsO_4 -catalyzed dihydroxylation under Upjohn conditions, furnishing bicyclic diols **55** with exclusive chemoselectivity of dihydroxylation at the less substituted olefin. Upon acetonide protection, the diol derivatives **56** were readily converted to dihydrodiols **57** through arenophile cycloreversion via one-pot hydrolysis of urazole moiety to afford a cyclic hydrazine, which was oxidized to the diazene, ultimately providing the corresponding diene following instantaneous expulsion of nitrogen. Alternatively, fragmentation of the arenophile moiety was achieved in a two-step protocol involving one-pot urazole hydrolysis and *bis*-benzoylation of the resulting hydrazine, followed by a reductive N–N cleavage using SmI_2 to afford diaminohydrodiol **58**. Benzene as well as other monosubstituted analogues with a wide variety of functional groups were tolerated in both processes, such as alkyl groups, benzylic heteroatoms, halogens, protected carbonyl groups, and silyl groups. In addition, polynuclear arenes were viable substrates (Scheme 15). Two concomitant one-pot procedures for the synthesis of diamino diol **60** were successfully conducted with naphthalene derivatives, heteroarenes, and phenanthrene.

This dearomative dihydroxylation protocol was applied towards the concise syntheses of natural products (Scheme 16). For example, conduramine A (**63**) was prepared from benzene-derived diol **61** through arenophile cycloreversion, nitroso-Diels-Alder reaction, and subsequent N–O cleavage.^[22] Furthermore, the syntheses of Amaryllidaceae alkaloids lycoricidine (**64**) and narciclasine (**65**) were accomplished from bromobenzene (**66**).^[23] In this case, dihydroxylation was conducted using the Narasaka-Sharpless modification of the Upjohn protocol, providing the dihydroxylated product in a form of boronic ester **68**. Utilizing the vinyl bromide and the arylboronic ester moiety of the compound **68**, a transpositive Suzuki coupling was then conducted to promote a key C–C bond formation (**69**). Further transformation into the isocarbostyryl framework **70** was achieved in a three-step sequence, which was then carried forward to provide lycoricidine (**64**) and narciclasine (**65**), respectively.

Similarly to oxidation, arenophile-mediated dearomative reduction was achieved by subjecting the arene-MTAD cycloadducts to *in situ* formed diimide (Scheme 17).^[24] The resulting reduced cycloadducts **71** could be further transformed into 1,3-cyclohexadienes **72**

or diaminocyclohexenes **73** through the same arenophile conversions described above. Noticeably, heteroatom groups at benzylic positions, as well as halogens, which are usually not compatible with other dearomative reductions, were tolerated under these conditions. When polynuclear arenes were employed, formal *bis*-1,4-hydroamination was achieved via two one-pot sequences: dearomative reduction, followed by hydrolysis of arenophile moiety and reductive N–N cleavage (Scheme 18). Moreover, the synthetic value of the dearomative reduction process was further demonstrated by converting the naphthalene-derived reduced cycloadduct **76** to a natural product γ -hydroxytetralone **77** and aminoalcohol **78**.

Olefin-like dearomative functionalization using arenophile-mediated dearomative hydroboration as a key step was also applied during the synthesis of idarubicinone (**82**), the aglycone of the FDA approved anthracycline idarubicin, by Sarlah and co-workers (Scheme 19).^[25] A multigram-scale Rh-catalyzed dearomative hydroboration of tetracenequinone derivative **79**, obtained from tetracene in two steps, with catecholborane proceeded smoothly to provide pinacol boronic ester **80**, which was then converted to a methyl ketone through reductive protection of the quinone moiety, followed by Zweifel olefination and hydrolysis. The resulting ketone **81** was converted to (\pm)-idarubicinone (**82**) in an additional four steps.

3.2. Transition-metal-catalyzed dearomative aminofunctionalization of arenes

Sarlah and co-workers demonstrated that arene-arenophile bicycles are also viable substrates for transition-metal-catalyzed ring-opening. This type of reactivity of the cycloadducts was expected, considering their strained nature and *bis*-allylic electron-deficient heteroatom sites, potentially prone to formal oxidative addition. The resulting organometallic intermediate could be captured with a variety of nucleophiles to afford the corresponding aminofunctionalized unsaturated products.

Accordingly, using Ni catalyst in combination with Grignard reagents as nucleophiles, carboamination of the corresponding arenes was achieved with exclusive *trans*-1,2-selectivity (Scheme 20).^[26] The reaction proceeded smoothly with aryl and vinyl Grignards, delivering carboaminated products of type **83** in high yields as well as high enantioselectivity for benzene and naphthalene (Conditions A). Additionally, substituted derivatives of benzene, naphthalene, as well as heteroarenes such as quinoline were viable substrates. To rationalize the regio- and stereochemical outcome of the reaction, the initial formation of η^5 -nickel cyclohexadienyl intermediate was proposed, undergoing inner-sphere reductive elimination mechanism to deliver *trans*-1,2-carboaminated products.^[26a]

Benzene-derived *trans*-1,2-carboaminated product **85** was uniquely suited for the enantioselective total synthesis of isocarbostryril alkaloids (Scheme 21). Having built the core carbon skeleton in a single step, as well as installed the requisite nitrogen- and carbon-based substituents on the aminocyclitol core with desired stereochemistry, (+)-7-deoxypancratistatin (**86**), (+)-pancratistatin (**87**), (+)-lycoricidine (**64**), and (+)-narciclasine (**65**) were synthesized in 6–7 steps from the key intermediate **85**.^[26a, 26c]

When using palladium catalysis, the arenophile-arene cycloadducts showed orthogonal regio- and stereoselectivity for the dearomative aminofunctionalization compared to nickel catalysis. For example, using naphthalene as a substrate with ketone- or ester-derived

lithium-enolates as nucleophiles, *syn*-1,4-selectivity was exclusively observed using both achiral and chiral ligands (Scheme 22, conditions A–C).^[27] Substituted naphthalenes, phenanthrene, and benzene were all suitable substrates in this transformation (Conditions A). Naphthalene-derived 1,4-carboaminated product could be further elaborated through olefin chemistry and urazole derivatizations to provide access to alicyclic motifs with various functional groups (Scheme 23).

Interestingly, when Grignard reagents were used in the presence of a palladium catalyst, exclusive *syn*-1,4-selectivity was observed (Scheme 24).^[28] Although the origin of this divergent regio- and stereoselectivity compared to the nickel-catalyzed system is unclear at this point, the reaction proceeded smoothly with benzene and a wide variety of Grignard reagents, including aryl, vinyl, and alkyl Grignards, using tri(*o*-methoxy)phosphine as a ligand. Moreover, monosubstituted benzene analogs as well as polynuclear arenes successfully underwent this dearomative carboamination when the ligand was changed to DPEphos. The synthetic utility of this process was demonstrated by converting naphthalene into Sertraline (**95**), one of the most prescribed antidepressants, in only four operations (Scheme 25), with potential application to enantioselective synthesis using (*S*)-DIFLUORPHOS (**97**).

In addition to carbon-based nucleophiles, also amines were competent nucleophiles for palladium-catalysis; the corresponding dearomative diamination delivered *syn*-1,4-diaminated products of type **98** (Scheme 26).^[29] With naphthalene as a substrate, both primary and secondary amines coupled smoothly under optimal conditions with achiral (Conditions A and B) as well as a chiral ligands (Conditions C). This transformation was also effective for substituted naphthalene, heteroarenes, and benzene.

4. Dearomatization via photochemically generated reactive radical intermediates

The Wang group has demonstrated the synthesis of *gem*-difluorinated spiro- γ -lactam oxindoles using indole substrates containing a C-3 bromodifluoroacetamide moiety (Scheme 27).^[30] Using [Ir(ppy)₃] as a catalyst under blue LED irradiation, the reaction proceeded smoothly to provide the corresponding 3,3'-spirocyclic oxindole **99** with both electron-withdrawing and electron-donating functional groups at various positions on the phenyl ring. As for the substituents at the two nitrogen atoms (R² and R³ groups), alkyl groups were well tolerated. Furthermore, while the reaction with unprotected indole (R² = H) proceeded with moderate yield, the desired product was not obtained when R³ was hydrogen.

The authors proposed that the reaction proceeds through a sequence of visible-light-induced difluoromethylative dearomatization, hydroxylation, and oxidation (Scheme 28). In the first step, photoexcited *[Ir(ppy)₃] reduced the bromodifluoroacetamide via a SET process to generate radical intermediate **100**, which underwent dearomatization through a 5-*exo* cyclization, furnishing indole C-2 radical species **101**. Oxidation of **101** by [Ir(ppy)₃]⁺ completed the photoredox catalytic cycle, and the resulting carbocation **102** was trapped by H₂O, followed by oxidation with PCC to afford the desired spirooxindole **103**.

The same group has also shown that this reaction system could be applied to a dearomatization/cyanation cascade process, in which 3,3'-spiroindolines with two contiguous quaternary carbon centers could be prepared (Scheme 29).^[31] The use of trimethylsilyl cyanide (TMSCN) as an external nucleophile successfully provided the corresponding *gem*-difluorinated and cyanated spiro- γ -lactam indolones **104**. In this method, substituents at indole N-1 and C-2 position (R^2 and R^3 group) were essential in providing the desired indolines in high diastereoselectivity. For example, when the R^3 group was larger than the methyl group, the product was obtained as a single diastereoisomer. On the other hand, when R^3 was a methyl group then bulkier R^2 groups were required for higher diastereoselectivity. Moreover, addition of hexafluoroisopropanol (HFIP, 10 eq.) played a crucial role for achieving the high yield of the desired product, most likely by contributing to the stabilization of the carbocation intermediate and circumventing unproductive side pathways, as suggested by the authors.

A first example for the synthesis of azaspirocyclic hexadienones from the corresponding *N*-(*p*-hydroxyphenyl)cinnamamides via photoredox catalytic dearomatization and radical cyclization was reported by Xia and co-workers in 2015 (Scheme 30).^[32] In this transformation, Togni's reagent was used as a trifluoromethyl source to initiate the process, in the presence of $[\text{Ir}(\text{ppy})_3]$ as a catalyst under blue LED visible-light conditions. At the same time, Zhu and co-workers reported a similar protocol using ethyl bromodifluoroacetate as a CF_2 radical precursor under visible-light irradiation, providing access to difluoroacetylated azaspiro[4.5]decane.^[33] In both scenarios, moderate to good yield of the desired azaspiro compounds were obtained, with or without the protection of phenol moiety.

In 2016, Dolbier and co-workers further expanded the arene scope of this transformation, and demonstrated a series of dearomative spirocyclizations of *N*-(*p*-hydroxybenzyl)acrylamides with various fluoroalkyl radical sources (Scheme 31).^[34] Using $[\text{Ir}(\text{ppy})_3]$ as a catalyst under visible light irradiation, difluoromethanesulfonyl chloride as well as other perfluoroalkyl sulfonyl chlorides effectively served as precursors for the CF_2H and perfluoroalkyl groups, providing the azaspiro compounds of type **105**. Different functional groups on the benzyl moiety (R^1) were well tolerated, and the use of alkyl groups as a *N*-substituent (R^2) proved essential for reaction to complete smoothly. The authors also showed the viability of 1-naphthol-derived substrates in this transformation. On the other hand, when $\text{FCH}_2\text{SO}_2\text{Cl}$ and $\text{CF}_3\text{CH}_2\text{SO}_2\text{Cl}$ were employed, the authors only observed product **106**, which retained the SO_2 group presumably due to the lower electronegativity of the FCH_2 and CF_3CH_2 groups required to expel SO_2 .^[35]

In all three cases above, similar reaction mechanisms were proposed (Scheme 32). Exemplified by the process developed by Dolbier, the reaction is initiated via reduction of the radical precursor (difluoromethanesulfonyl chloride) by a photoexcited $^*[\text{Ir}(\text{ppy})_3]$, followed by the addition of the radical species HCF_2 to the acrylamide **107**. The resulting radical intermediate **108** then engages in a dearomative 5-*exo* cyclization into the benzyl moiety, and subsequent oxidation by $[\text{Ir}(\text{ppy})_3]^+$ generated carbocation **110** as well as regenerated the catalyst. Finally, the product **111** was formed upon reaction with water under basic conditions.

The dearomative radical cyclization strategies for the formation of spirocyclic scaffolds with phenols have found several applications. For example, Zhang and co-workers replaced the acrylamide moiety of the *N*-(*p*-hydroxybenzyl)acrylamide with α -bromo-alkylamide to synthesize azaspiro[4.5]decane **112** (Scheme 33).^[36] While various protecting groups on the amide nitrogen (R^1 group) such as *tert*-butyl group, $\text{CH}_2\text{CO}_2\text{Me}$, and benzyl groups were tolerated, the reaction did not proceed with the unprotected amide ($R^1 = \text{H}$). Additionally, α -substituents next to the carbonyl group (R^2, R^3) had a minor impact on the reaction outcome. Although majority of the examples were performed with phenol derivatives, the authors demonstrated that naphthol was also a viable substrate for this dearomative photocyclization.

Intermolecular dearomative radical cyclization for the synthesis of spirocarbocycles was also developed by Zhang and co-workers (Scheme 34).^[37] In this transformation, an α -diketo radical formed by reduction of the α -bromide with photoexcited $^*[\text{Ir}(\text{ppy})_3]$, underwent addition to an alkyne, and subsequent 5-exo spirocyclization formed spiro[4,5]decane **113**. The alkyne scope turned out to be broad; both terminal and internal alkynes bearing a wide variety of functional groups were good substrates for this process. Notably, while most of the alkynes gave rise to the product with the substituent at the α -position of the newly formed spirocarbon center, propiophenone exhibited reversed regioselectivity. With regard to the arene scope, both phenol and naphthol derivatives were readily dearomatized under these conditions.

Although less developed, arenes other than indole derivatives and phenolic compounds have also been applied in the photochemical dearomatization processes in a similar fashion. For instance, visible-light-mediated synthesis of spirodihydrofuranols from 2-furan carboxyamides bearing photoredox active *N*-acyloxyphthalimides was recently demonstrated by Reiser and co-workers (Scheme 35A).^[38] Alternatively, spirobutenolides could be prepared directly when bromide functionality was introduced at C-5 position of furan (Scheme 35B). In both cases, the use of $[\text{Ir}(\text{ppy})_2(\text{dtbbpy})\text{PF}_6]$ (**22**) as a photoredox catalyst under blue LED light irradiation gave the best results, and the reaction showed good functional group tolerance, albeit with erosion in diastereoselectivity.

The utility of this dearomatization was demonstrated with the formal synthesis of (*S*)-(+)-lycoperdic acid (Scheme 36). Furan derivative **114**, which was readily prepared from 5-bromofurfural and (*S*)-aspartic acid dimethyl ester, was subjected to a dearomative photocyclization to effectively construct a spirobutenolide fused to pyrrolidine (**115**). Subsequent hydrogenation provided the butyrolactone **116**, which could be further transformed to (*S*)-(+)-lycoperdic acid (**117**) by a route described by Yoshifuji.^[39]

Zhang and co-workers expanded their previously reported approach to intermolecular dearomative cyclization of 2-bromofurans (Scheme 37). Upon formation of an α -carbon radical intermediate by the photoredox catalyst, a range of alkynes were incorporated, forming the corresponding spirobutenolides **118**.^[40]

Finally, a visible-light-mediated dearomative spirocyclization of non-phenolic biaryl compounds was described by Wang, Samec, and co-workers (Scheme 38).^[41] The reaction

was driven by the formation of carboxyl radical **120** using acridinium catalyst under aerobic conditions, and subsequent dearomative cyclization delivered cyclohexadienyl radical **121**, which underwent capture with triplet oxygen (**121**→**122**, Scheme 38B). Subsequent fragmentation (**122**→**123**) and TEMPO oxidation delivered desired product **124**.

Importantly, the reaction proceeded smoothly with a variety of biaryl compounds, including substrates bearing a pyridine moiety (Scheme 38C).

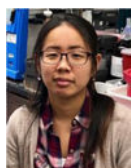
5. Summary and outlook

The field of visible-light-mediated dearomatization has seen major advancement in recent years. As showcased in this review, numerous methods have been developed to successfully activate a range of arenes and heteroarenes under mild conditions, providing access to unique and complex alicyclic scaffolds from readily available precursors. Despite the expansive impact these processes have had on the dearomative synthetic toolbox, there is still ample uncharted reaction space for further developments and improvements. For example, majority of transformations are still limited to activated arenes, such as indoles and naphthols. Increasing the number of methods applicable to non-activated arenes, such as simple benzene and naphthalene derivatives, would greatly benefit in expanding the scope and utility of such processes. Moreover, enantioselective, visible-light-mediated dearomative transformations are rare and there is a strong need in further advancement of this area. Nevertheless, these new promising approaches provide confidence for the future discovery of even more effective uses of simple aromatic compounds for the synthesis of complex molecules in organic synthesis.

Acknowledgments

We would like to acknowledge the University of Illinois, Petroleum Research Fund (PRF#57175-DNI1), the National Science Foundation (CAREER Award No. CHE-1654110), and the NIH/National Institute of General Medical Sciences (R01 GM122891) for the support. D. S. is an Alfred P. Sloan Fellow. M. O. acknowledges the Honjo International Scholarship Foundation.

Biographies



Mikiko Okumura was born and raised in Japan. She received her B.S. (2012) and M.S. (2014) in chemistry at The University of Tokyo working with Professor Shu Kobayashi. She then pursued her graduate studies in the Sarlah group at the University of Illinois at Urbana-Champaign, where she obtained her Ph.D. (2019) by developing new dearomatization strategies using arenophiles. Currently she is a JSPS postdoctoral fellow in the laboratory of Professor Thomas J. Maimone at UC Berkeley.

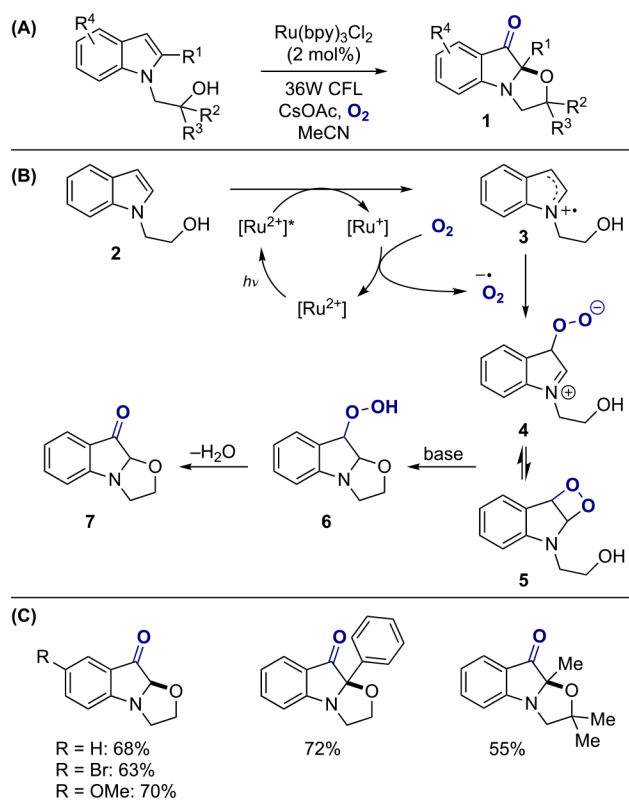


David Sarlah is an assistant professor in the Department of Chemistry at the University of Illinois at Urbana-Champaign. He was born in Slovenia, where he earned his B.S. degree from the University of Ljubljana. He obtained his Ph.D. in 2011 with Professor K. C. Nicolaou at The Scripps Research Institute, and then joined the laboratory of Professor Erick M. Carriera at ETH Zurich. In 2014, David returned to the States to start his own laboratory, which explores both chemical synthesis of biologically active natural products and method development.

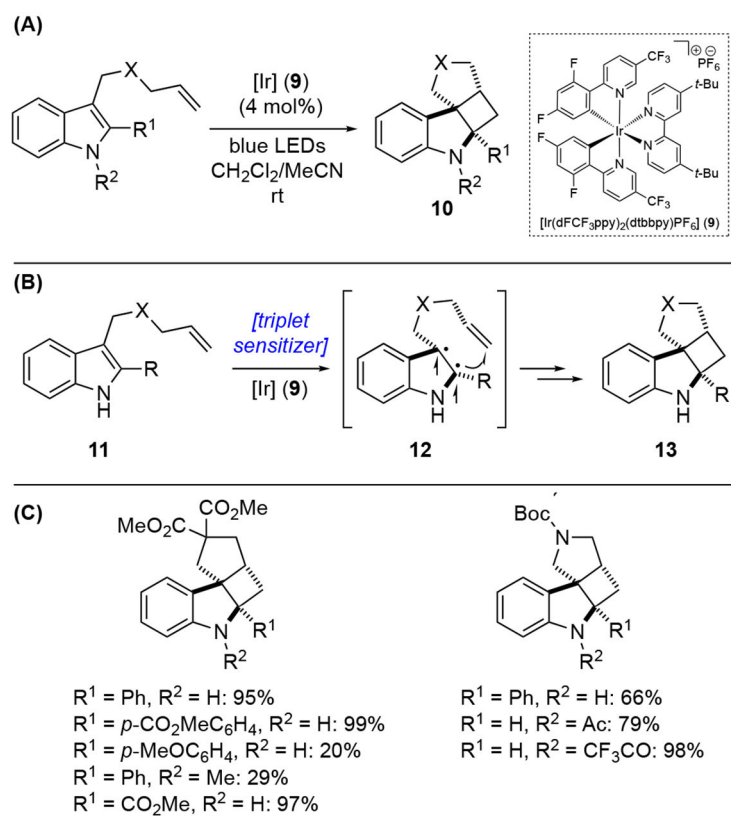
References

- [1]. Foubelo F, Yus M in *Arene Chemistry: Reaction Mechanisms and Methods for Aromatic Compounds*, ed. Mortier J, John Wiley-VCH: Weinheim, 2015.
- [2]. a)Roche SP, Porco JA Jr., *Angew. Chem., Int. Ed.*, 2011, 50, 4068–4093;b)Asymmetric Dearomatization Reactions. Ed. You S-L, Wiley-VCH, 2016;c)Wertjes WC, Southgate EH, Sarlah D, *Chem. Soc. Rev* 2018, 47, 7996–8017. [PubMed: 30073226]
- [3]. Rabideau PW, Marcinow Z, *Org. React* 1992, 42, 1–334.
- [4]. a)Dyson PJ, *Dalton Trans*, 2003, 2964–2974;b)Gualandi A, Savoia D, *RSC Adv.*, 2016, 6, 18419–18451;c)Wiesefeldt MP, Nairoukh Z, Dalton T, Glorius F, *Angew. Chem. Int. Ed* 2019, 58, 10460–10476.
- [5]. a)Pouységu L, Deffieux D, Quideau S, *Tetrahedron*, 2010, 66, 2235–2261;b)Ding Q, Ye Y, Fan R, *Synthesis*, 2013, 1–16;c)Wu W-T, Zhang L, You S-L, *Chem. Soc. Rev*, 2016, 45, 1570–1580. [PubMed: 26796922]
- [6]. a)Pape AR, Kaliappan KP, Kündig EP, *Chem. Rev*, 2000, 100, 2917–2940; [PubMed: 11749310] b)Rosillo M, Dominguez G, Pérez-Castells J, *Chem. Soc. Rev*, 2007, 36, 1589–1604; [PubMed: 17721584] c)Liebov BK, Harman WD, *Chem. Rev*, 2017, 117, 13721–13755. [PubMed: 29064228]
- [7]. For example:a)McCullough JJ, *Chem. Rev* 1987, 87, 811–860;b)Bryce-Smith D, Gilbert A, *Tetrahedron*, 1976, 32, 1309–1326;c)Bryce-Smith D, Gilbert A, *Tetrahedron*, 1977, 33, 2459–2489.
- [8]. a)Remy R, Bochet CG, *Chem. Rev*, 2016, 116, 9816–9849; [PubMed: 27340900] b)Streit U, Bochet CG, *Beilstein J. Org. Chem*, 2011, 7, 525–542. [PubMed: 21647263]
- [9]. a)Prier CK, Rankic DA, *MacMillan DWC*, *Chem. Rev* 2013, 113, 5322–5363; [PubMed: 23509883] b)Romero NA, Nicewicz DA, *Chem. Rev* 2016, 116, 10075–10166. [PubMed: 27285582]
- [10]. Zhang M, Duan Y, Li W, Cheng Y, Zhu C, *Chem. Commun* 2016, 52, 4761–4763.
- [11]. Zhu M, Zheng C, Zhang X, You S-L, *J. Am. Chem. Soc* 2019, 141, 2636–2644. [PubMed: 30653315]
- [12]. Cheng Y-Z, Zhou K, Zhu M, Li L-A-C, Zhang X, You S-L, *Chem. Eur. J* 2018, 24, 12519–12523. [PubMed: 29932260]
- [13]. James MJ, Schwarz JL, Strieth-Kalthoff F, Wibbeling B, Glorius F, *J. Am. Chem. Soc* 2018, 140, 8624–8628. [PubMed: 29961335]
- [14]. Stegbauer S, Jandl C, Bach T, *Angew. Chem. Int. Ed* 2018, 57, 14593–14596.
- [15]. Hu N, Jung H, Zheng Y, Lee J, Zhang L, Ullah Z, Xie X, Harms K, Baik M-H, Meggers E, *Angew. Chem. Int. Ed* 2018, 57, 6242–6246.
- [16]. Zhu M, Zhou K, Zhang X, You S-L, *Org. Lett* 2018, 20, 4379–4383. [PubMed: 29985618]
- [17]. Guo Q, Wang M, Liu H, Wang R, Xu Z, *Angew. Chem. Int. Ed* 2018, 57, 4747–4751.

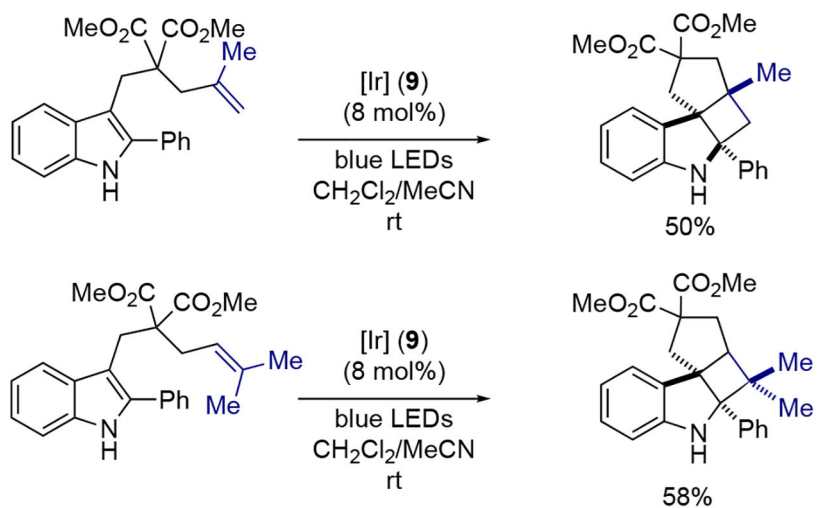
- [18]. Okumura M, Sarlah D, Synlett, 2018, 29, 845–855.
- [19]. Bruycker KD, Billiet S, Houck HA, Chattopadhyay S, Winne JM, Du Prez FE, Chem. Rev 2016, 116, 3919–3974. [PubMed: 26900710]
- [20]. a)Kjell DP, Sheridan RS, J. Am. Chem. Soc, 1984, 106, 5368–5370;b)Hamrock SV, Sheridan RS, J. Am. Chem. Soc 1989, 111, 9247–9249.
- [21]. See reference 20 and references therein.
- [22]. Southgate EH, Pospech J, Fu J, Holycross DR, Sarlah D, Nat. Chem, 2016, 8, 922–928. [PubMed: 27657867]
- [23]. Southgate EH, Holycross DR, Sarlah D, D. Angew. Chem. Int. Ed 2017, 56, 15049–15052.
- [24]. Okumura M, Nakamata Huynh SM, Pospech J, Sarlah D, Angew. Chem. Int. Ed 2016, 55, 15910–15914.
- [25]. Dennis DG, Okumura M, Sarlah D, J. Am. Chem. Soc 2019, 141, 10193–10198. [PubMed: 31244190]
- [26]. a)Hernandez LW, Pospech J, Klöckner U, Bingham TW, Sarlah D J. Am. Chem. Soc 2017, 139, 15656–15659; [PubMed: 29059521] b)Hernandez LW, Klöckner U, Pospech J, Hauss L, Sarlah D, J. Am. Chem. Soc 2018, 140, 4503–4507; [PubMed: 29544244] c)Bingham TW, Hernandez LW, Olson DG, Svec RL, Hergenrother PJ, Sarlah D, J. Am. Chem. Soc 2019, 141, 657–670. [PubMed: 30520639]
- [27]. Okumura M, Shved AS, Sarlah D, J. Am. Chem. Soc 2017, 139, 17787–17790. [PubMed: 29183109]
- [28]. Tang C, Okumura M, Zhu Y, Hooper A, Zhou Y, Lee Y, Sarlah D, Angew. Chem. Int. Ed 2019, 58, 10245–10249.
- [29]. Wertjes WC, Okumura M, Sarlah D, J. Am. Chem. Soc 2019, 141, 163–167. [PubMed: 30566338]
- [30]. Wang Q, Qu Y, Xia Q, Song H, Song H, Liu Y, Wang Q, Chem. Eur. J 2018, 24, 11283–11287. [PubMed: 29797623]
- [31]. Wang Q, Qu Y, Xia Q, Song H, Song H, Liu Y, Wang Q, Adv. Synth. Catal 2018, 360, 2879–2884.
- [32]. Gao F, Yang C, Gao G-L, Zheng L, Xia W, Org. Lett 2015, 17, 3478–3481. [PubMed: 26126702]
- [33]. Gu Z, Zhang H, Xu P, Cheng Y, Zhu C, Adv. Synth. Catal 2015, 357, 3057–3063.
- [34]. Zhang Z, Tang X-J, Dolbier WR Jr. Org. Lett 2016, 18, 1048–1051. [PubMed: 26866977]
- [35]. For more substrate scope using C4F9SO2Cl, see:Tang S, Yuana L, Lia Z-Z, Penga Z-Y, Denga Y-L, Wanga L-N, Huanga G-X, Sheng R-L, Tetrahedron Lett. 2017, 58, 2127–2130.
- [36]. Hu B, Li Y, Dong W, Ren K, Xie X, Wan J, Zhang Z, Chem. Commun 2016, 52, 3709–3712.
- [37]. Dong W, Yuan Y, Gao X, Keranmu M, Li W, Xie X, Zhang Z, Org. Lett 2018, 20, 5762–5765. [PubMed: 30192154]
- [38]. Kachkovskiy G, Faderl C, Reiser O, Adv. Synth. Catal 2013, 355, 2240–2248.
- [39]. Yoshifuji S, Kaname M, Chem. Pharm. Bull 1995, 43, 1617–1620.
- [40]. Dong W, Yuan Y, Gao X, Keranmu M, Li W, Xie X, Zhang Z, J. Org. Chem 2019, 84, 1461–1467. [PubMed: 30605614]
- [41]. Li H, Subbotina EBunrit A, Wang F, Samec JSM, Chem. Sci 2019, 10, 3681–3686. [PubMed: 30996963]

**Scheme 1.**

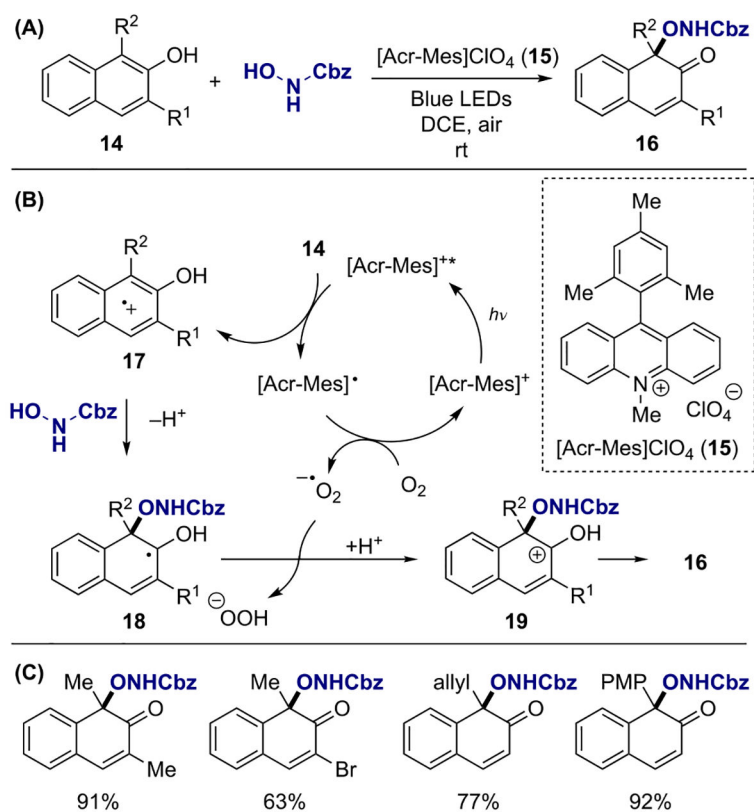
Visible-light-mediated aerobic dearomatization of indoles: (a) general reaction; (b) proposed mechanism; (c) substrate scope.

**Scheme 3.**

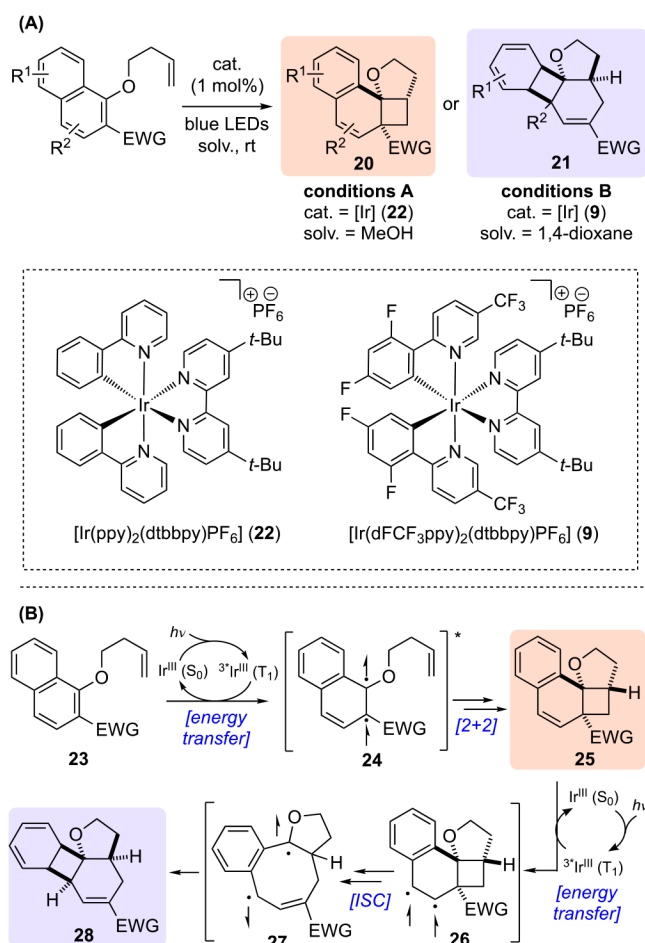
Visible-light-promoted dearomatization and [2+2] cycloaddition: (a) general reaction; (b) proposed mechanism; (c) substrate scope.

**Scheme 4.**

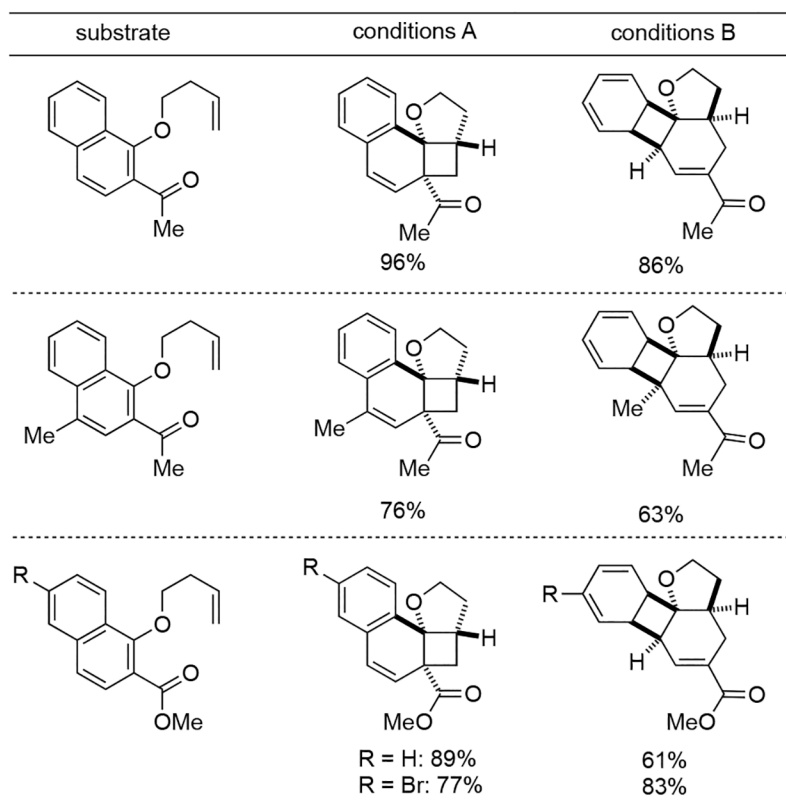
Synthesis of tetracyclic spiroindolines bearing all-carbon quaternary stereogenic centers.

**Scheme 5.**

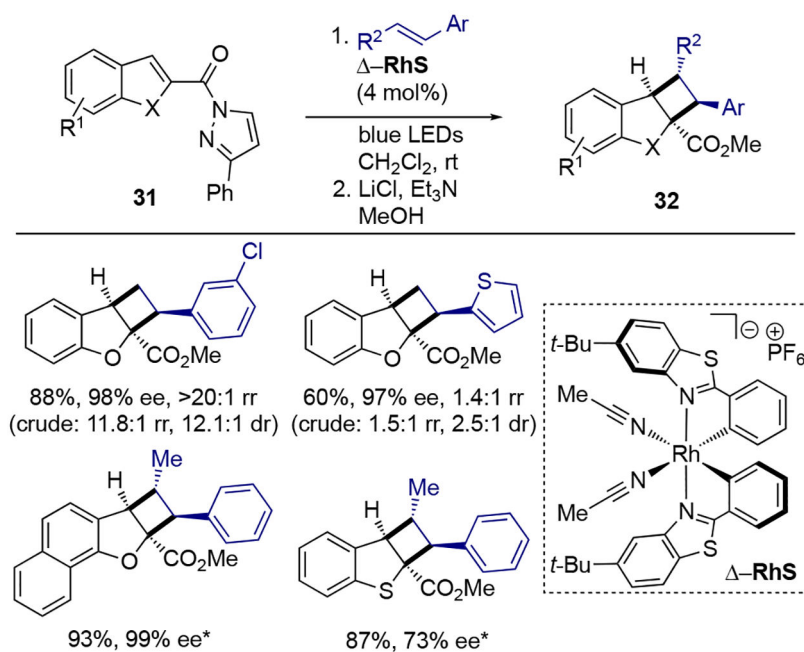
Visible-light-promoted intermolecular oxidative dearomatization of 2-naphthols: (a) general reaction; (b) proposed mechanism; (c) substrate scope.



Scheme 6. Dearomative cascade photocatalysis of 1-naphthols: (a) general reaction; (b) proposed mechanism.

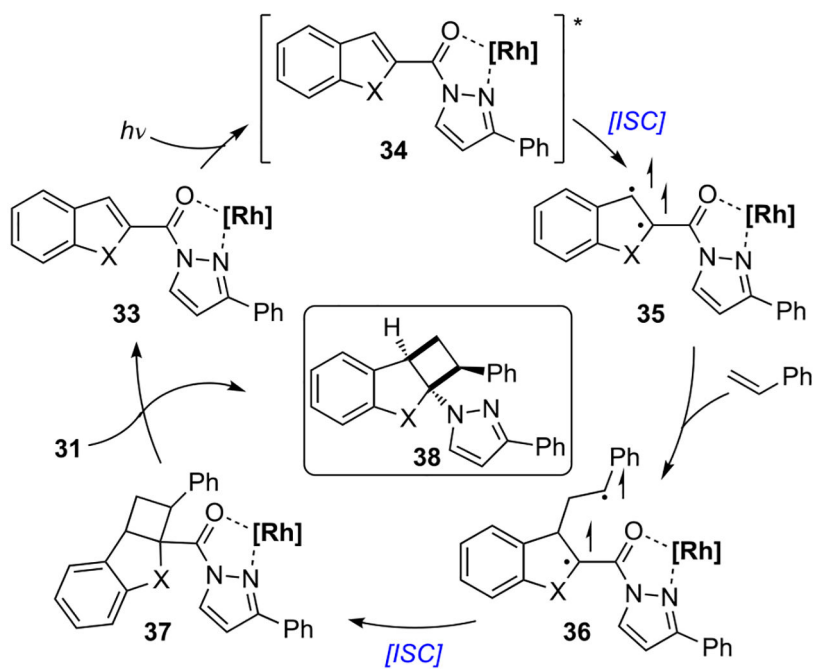
**Scheme 7.**

Scope of dearomative cascade photocatalysis with 1-naphthol derivatives.

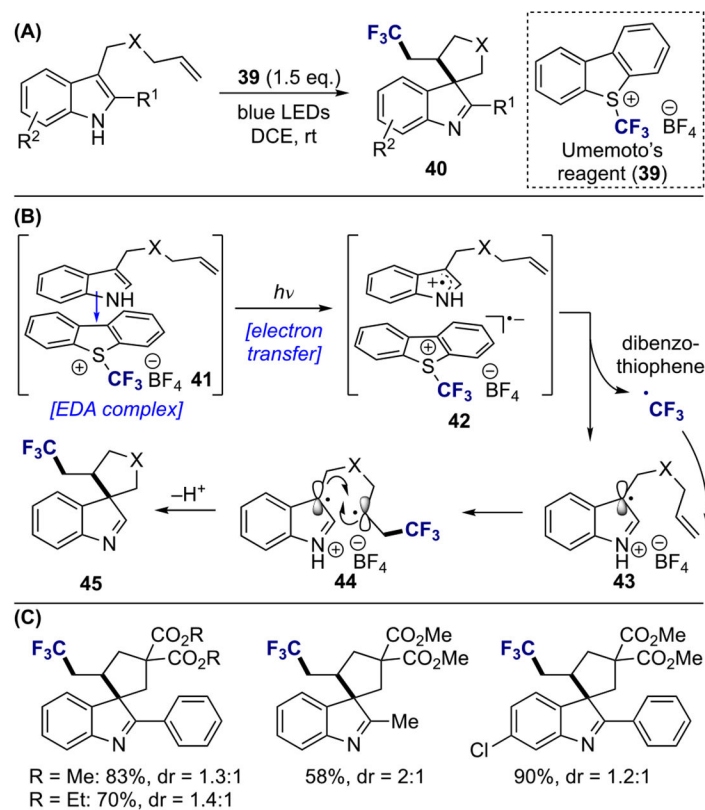
**Scheme 9.**

Catalytic asymmetric dearomatization through visible-light-promoted [2+2] photocycloaddition.

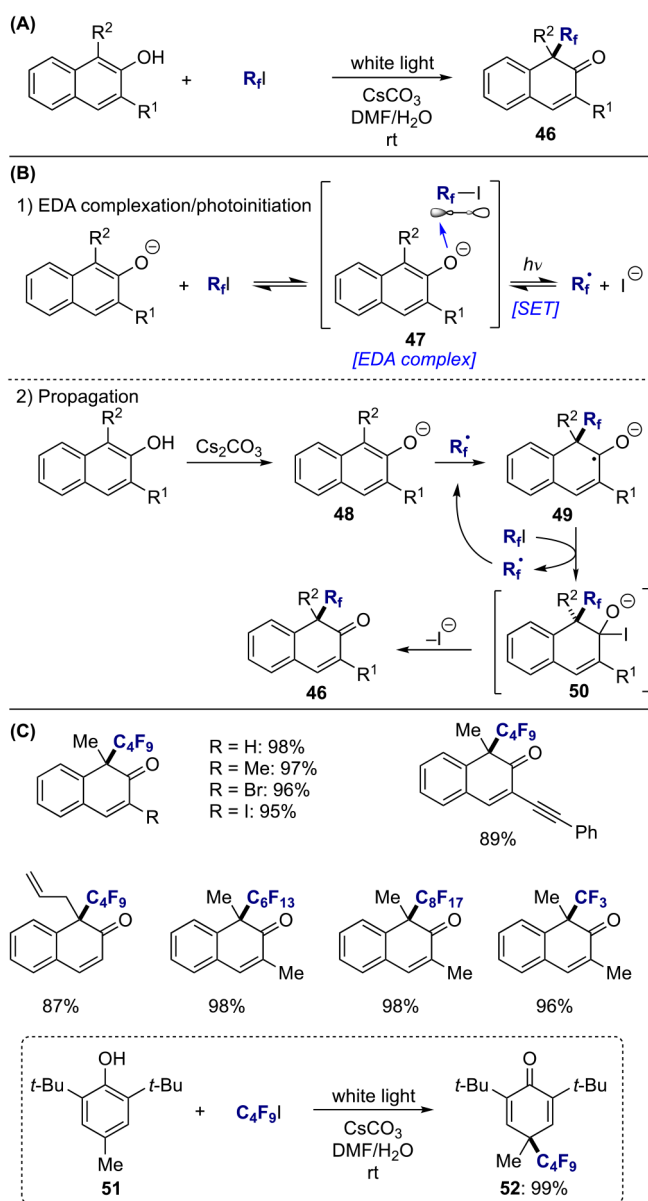
* Single diastereo- and constitutional isomer was observed.



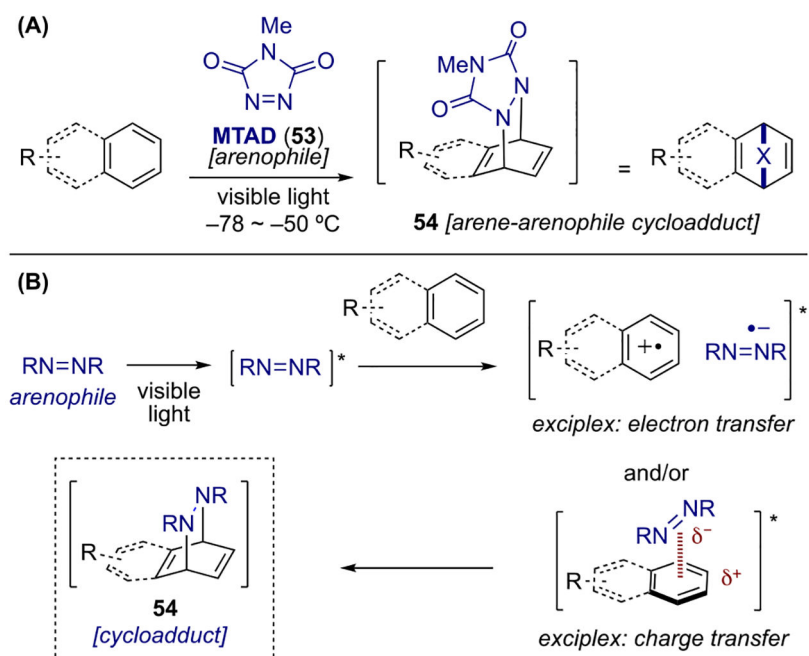
Scheme 10.
Proposed mechanism of visible-light-promoted [2+2] photocycloaddition.

**Scheme 11.**

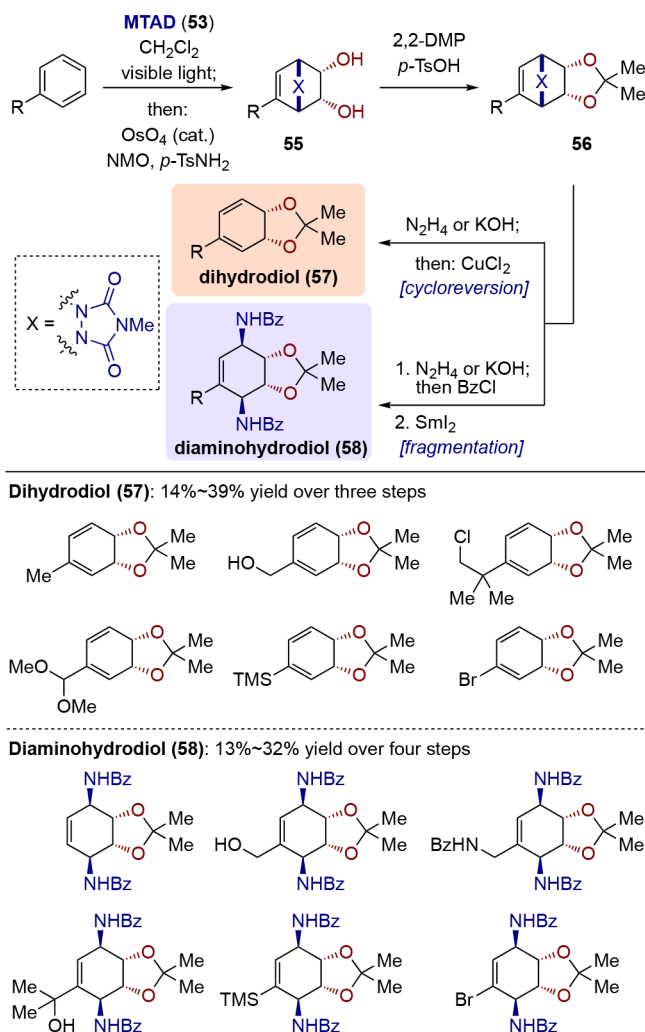
Visible-light-promoted dearomative cascade alkene trifluoromethylation: (a) general reaction; (b) proposed mechanism; (c) substrate scope.

**Scheme 12.**

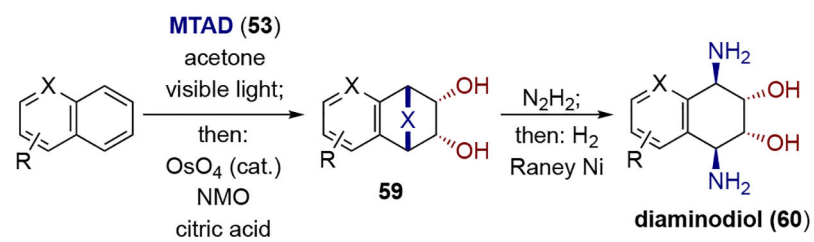
Visible-light-promoted dearomative fluoroalkylation of 2-naphthols: (a) general reaction; (b) proposed mechanism; (c) scope.

**Scheme 13.**

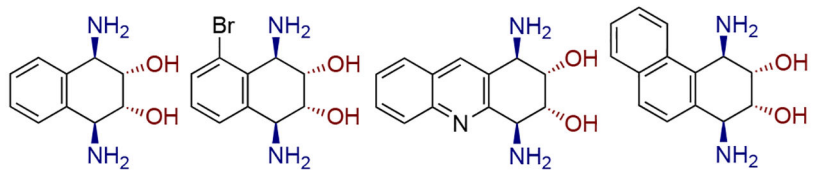
Arenophile-mediated dearomatization: (a) general reaction; (b) proposed mechanism.



Scheme 14. Arenophile-mediated dearomative dihydroxylation and product derivatizations.

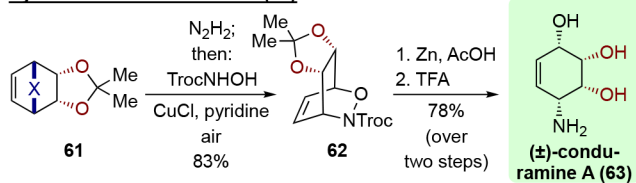
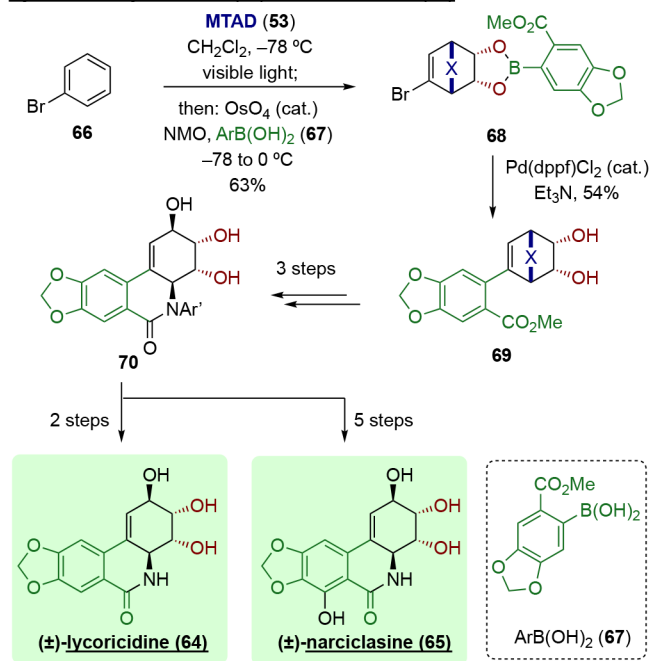


Diaminodiol (60): 21%~63% yield over two steps

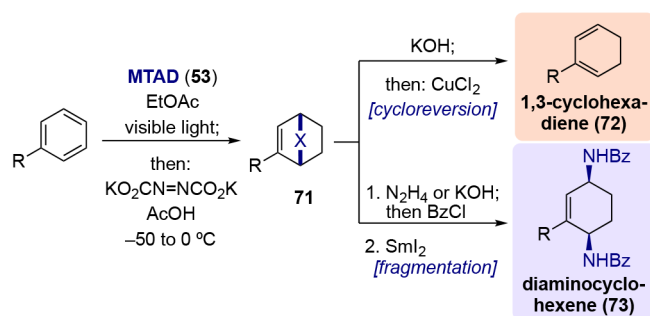


Scheme 15.

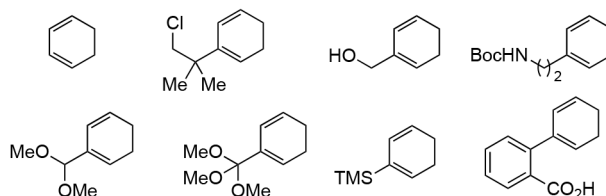
Arenophile-mediated dearomative dihydroxylation and arenophile fragmentation of polynuclear arenes.

Synthesis of conduramine A (63)**Synthesis of lycoricidine (64) and narciclasine (65)****Scheme 16.**

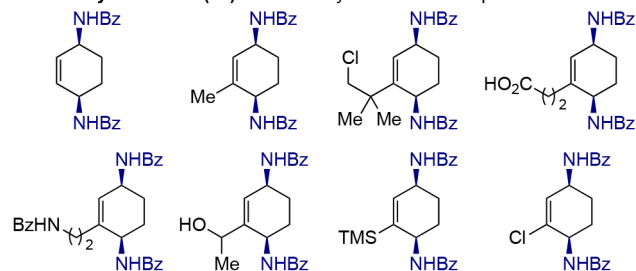
Representative synthesis applications of dearomative dihydroxylation.



1,3-cyclohexadiene (72): 35%~67% yield over two steps

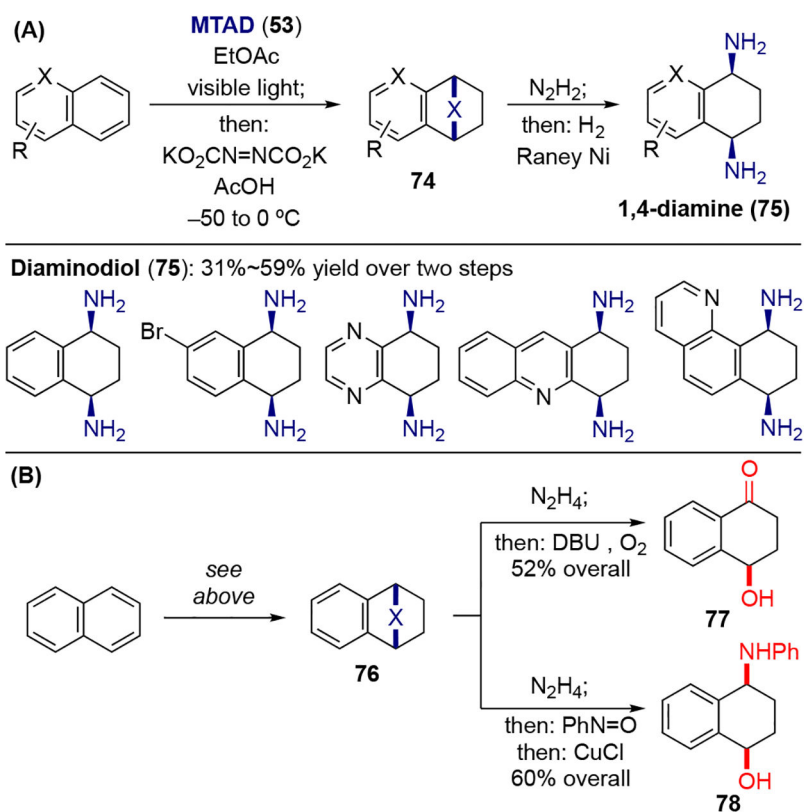


Diaminocyclohexene (73): 14%~39% yield over four steps

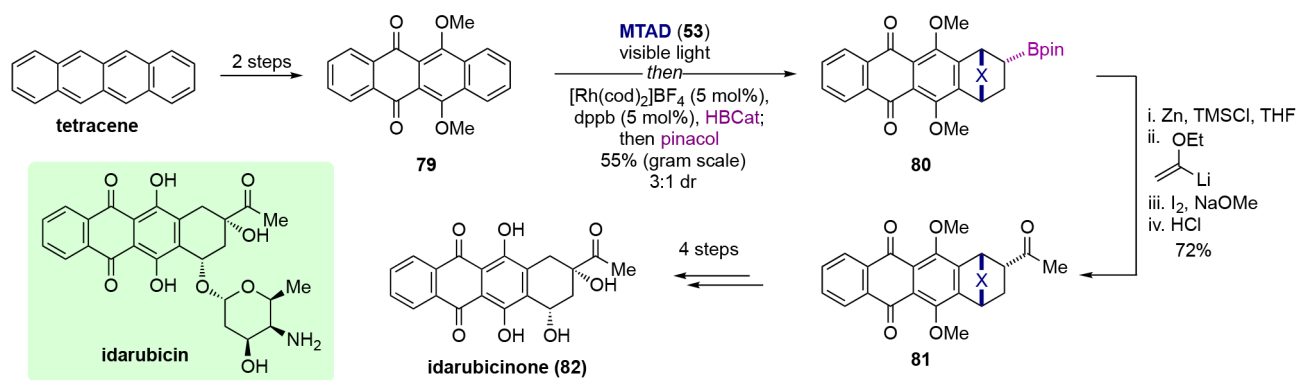


Scheme 17.

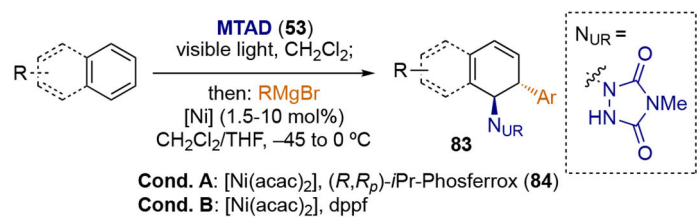
Arenophile-mediated dearomative reduction and product derivatizations.

**Scheme 18.**

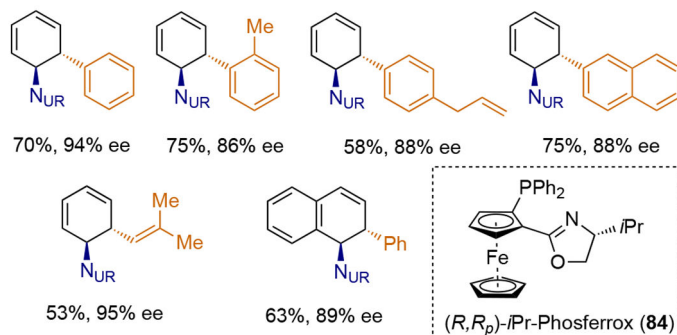
Arenophile-mediated dearomative reduction of polynuclear arenes: a) synthesis of bis-1,4-hydroaminated arenes; b) derivatizations.

**Scheme 19.**

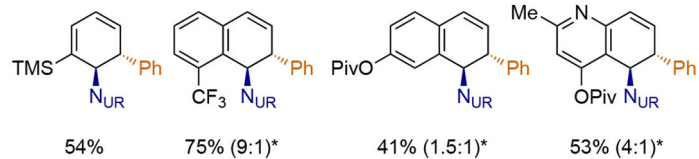
Synthesis of idarubicinone(82) through areophile-mediated dearomative hydroboration.



Cond. A:



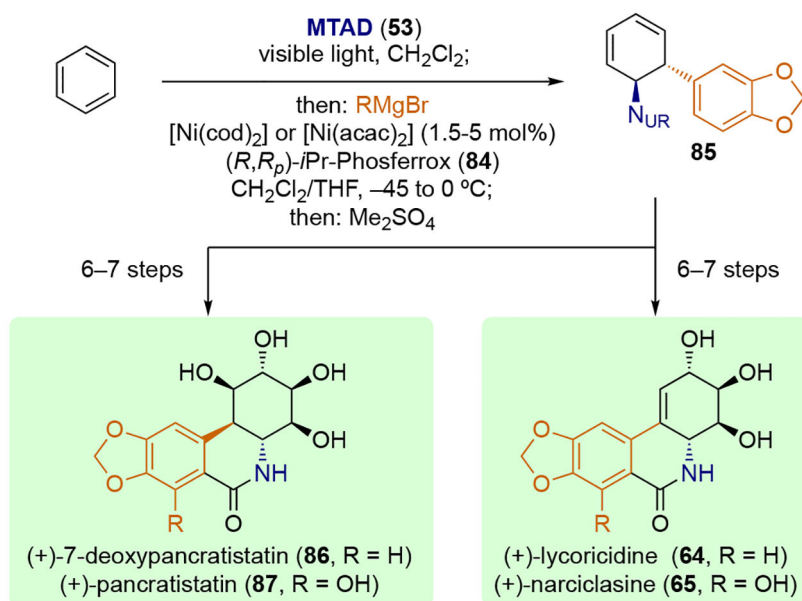
Cond. B:



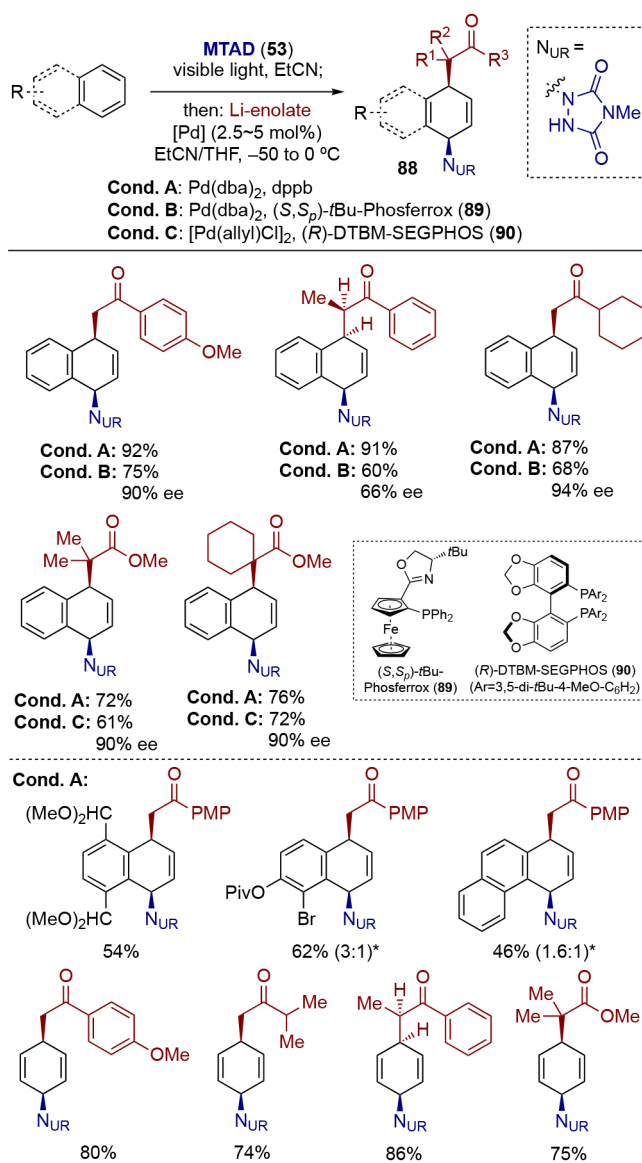
Scheme 20.

Nickel-catalyzed dearomative *trans*-1,2-carboaminations.

* Ratio of constitutional isomers are shown in parenthesis.

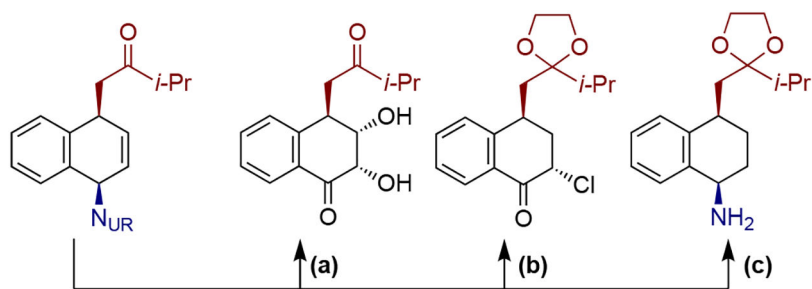
**Scheme 21.**

Applications to the enantioselective total syntheses of isocarbostyryl alkaloids.

**Scheme 22.**

Palladium-catalyzed dearomative *syn*-1,4-carboamination with enolate nucleophiles.

* Ratio of constitutional isomers are shown in parenthesis.



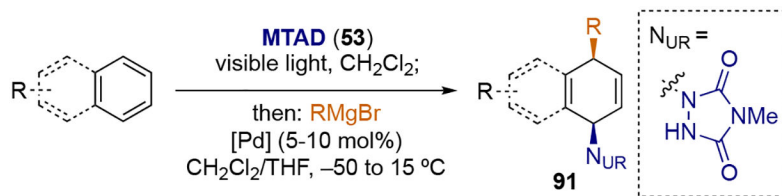
(a) i. OsO₄ (cat.), NMO, 87%; ii. NaOCl, 40%.

(b) i. Rh/Al₂O₃ (cat.), H₂, 93%; ii. glycol, 85%; iii. ^tBuOCl, 72%.

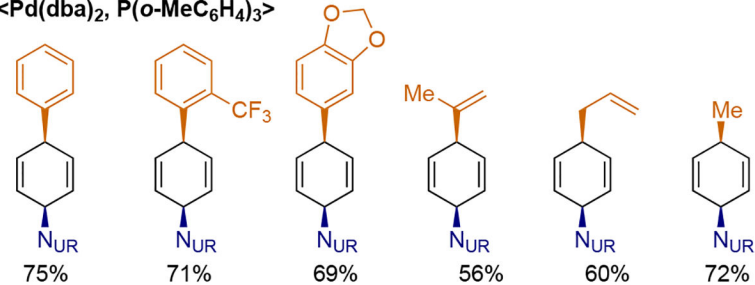
(c) i. Rh/Al₂O₃ (cat.), H₂, 93%; ii. glycol, 85% iii. α -Br-acetophenone, NaH, 78%; iv. KOH, 97%.

Scheme 23.

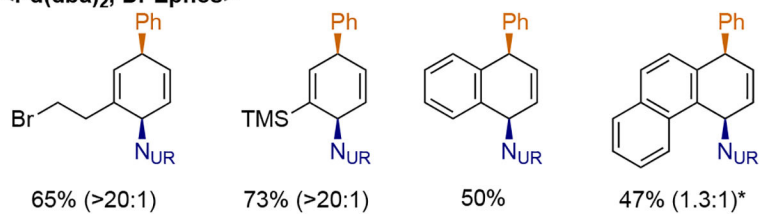
Elaborations of *syn*-1,4-carboaminated naphthalene.



<Pd(dba)₂, P(o-MeC₆H₄)₃>



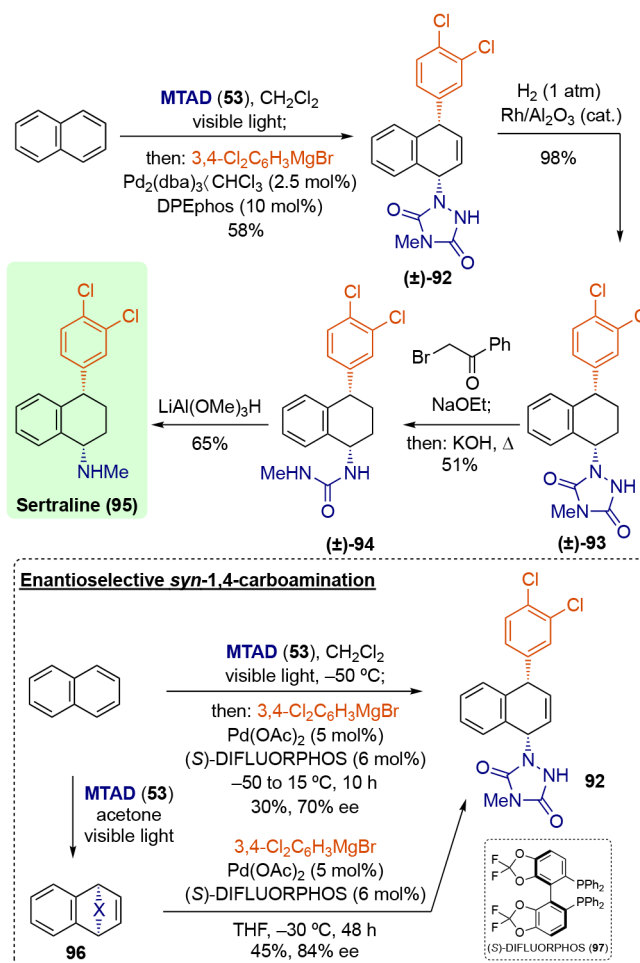
<Pd(dba)₂, DPEphos>



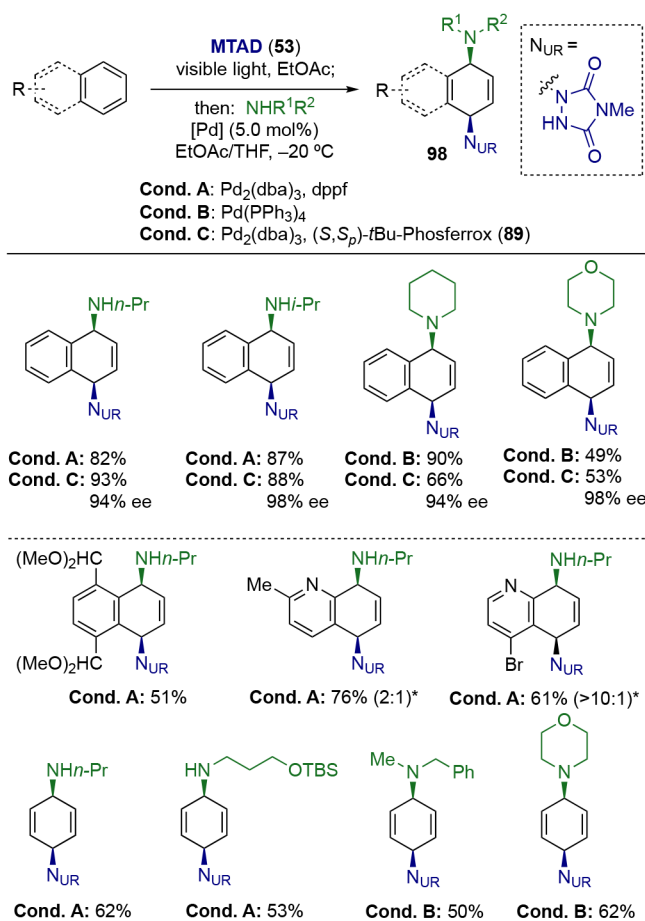
Scheme 24.

Palladium-catalyzed dearomative *syn*-1,4-carboamination with Grignard reagents.

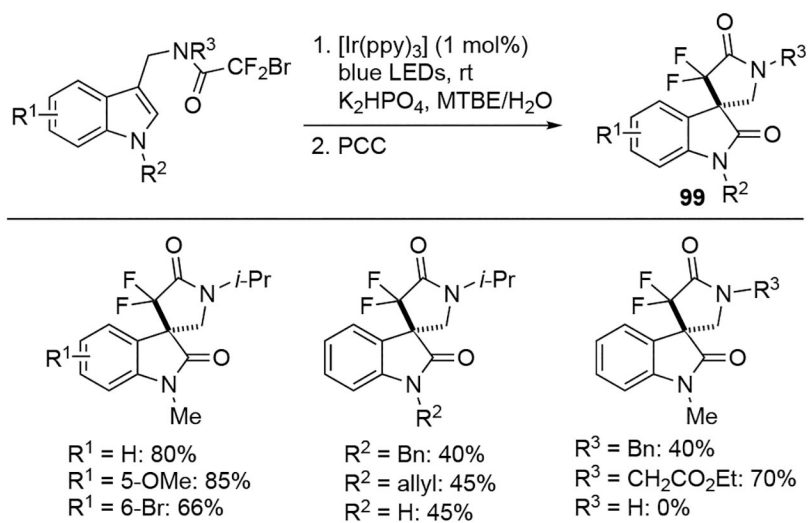
* Ratio of constitutional isomers are shown in parenthesis.

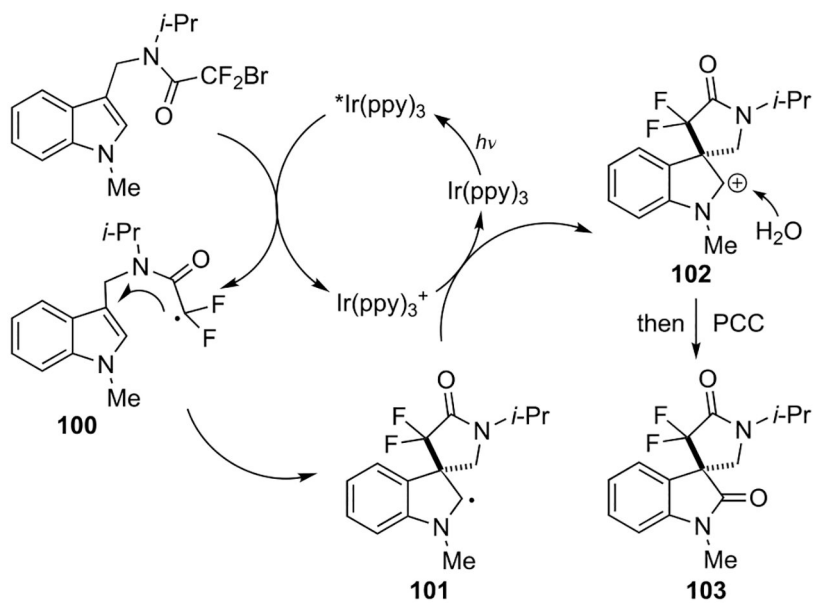


Scheme 25.
Synthesis of sertraline (95).

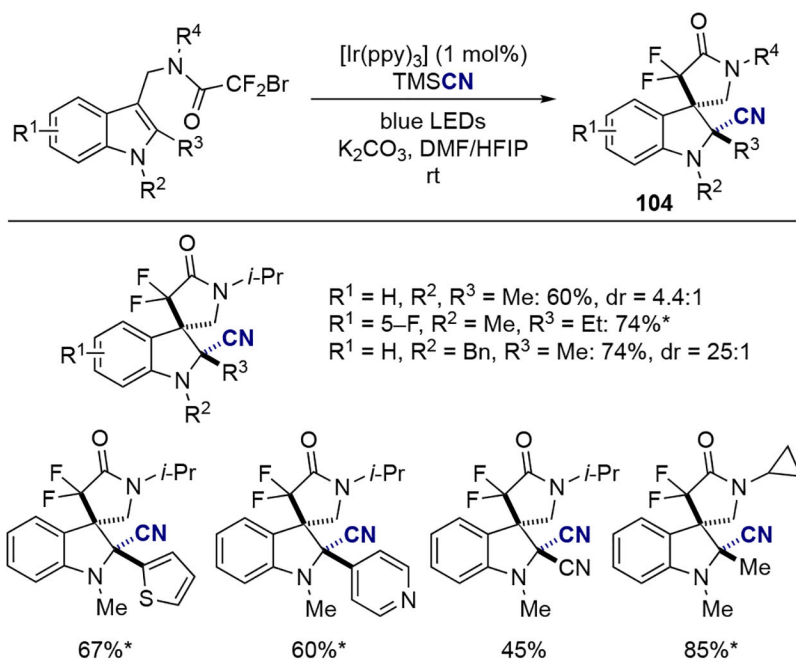
**Scheme 26.**Palladium-catalyzed dearomative *syn*-1,4-diaminations.

* Ratio of constitutional isomers are shown in parenthesis.

**Scheme 27.**Synthesis of of *gem*-difluorinated spiro- γ -lactam oxindoles.

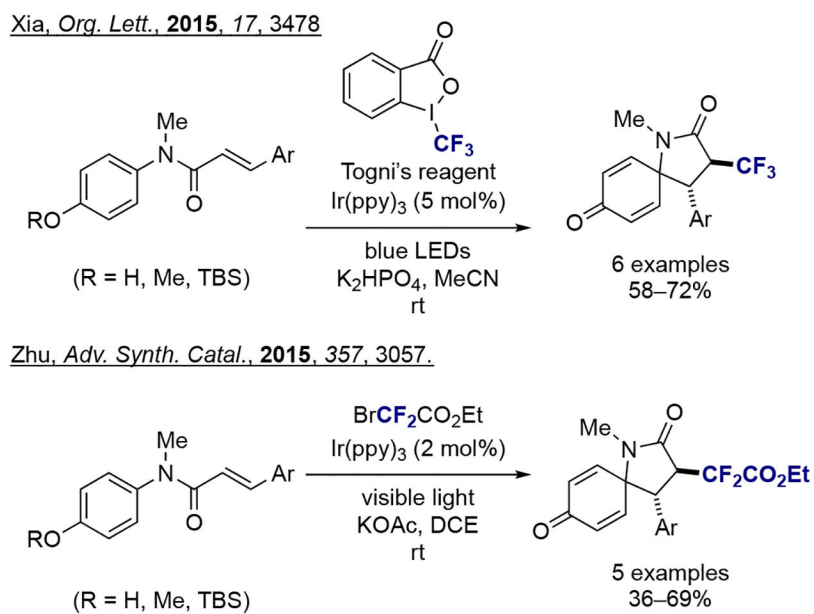


Scheme 28.
Proposed reaction mechanism.

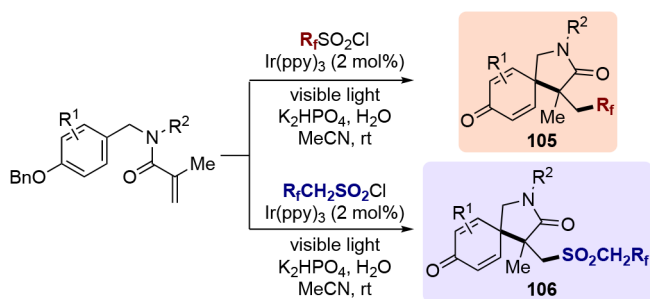
**Scheme 29.**

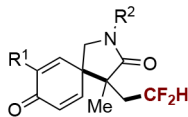
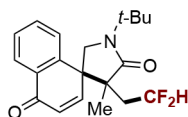
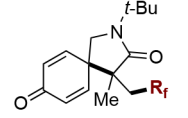
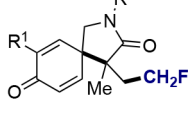
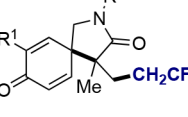
Dearomatization/cyanation cascade of indole derivatives.

*Single diastereoisomer was observed.

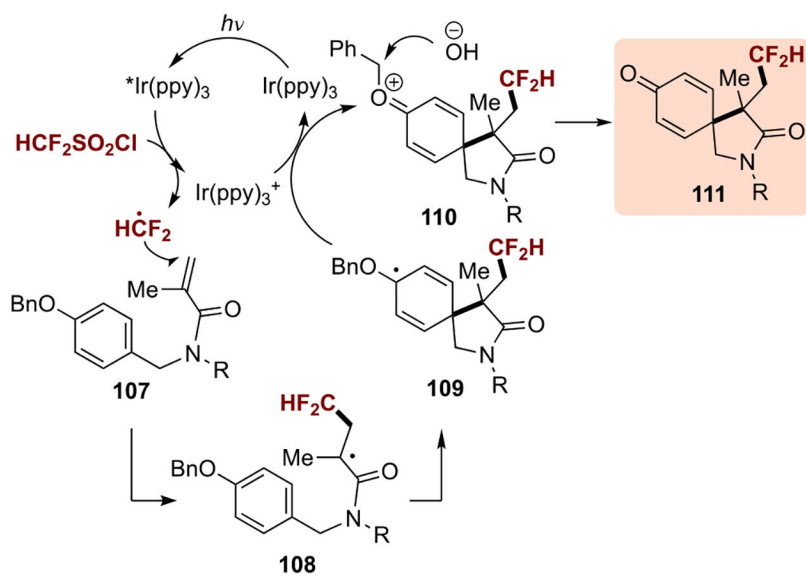
**Scheme 30.**

Photoredox catalytic dearomatization and radical cyclization for the synthesis of azaspirocyclic hexadienones.

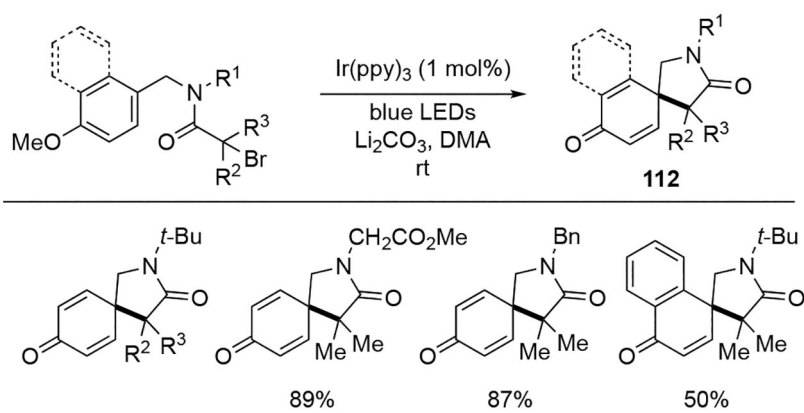


R_fSO_2Cl or $R_fCH_2SO_2Cl$	product
HCF_2SO_2Cl	 $R^1 = H, R^2 = t\text{-Bu}: 82\%$ $R^1 = H, R^2 = Bn: 82\%$ $R^1 = OMe, R^2 = t\text{-Bu}: 76\%$ $R^1 = Cl, R^2 = t\text{-Bu}: 84\%$
providing HCF_2SO_2Cl	 78%
R_fSO_2Cl	 $R_f = CF_3: 88\%$ $R_f = C_4F_9: 85\%$
FCH_2SO_2Cl	 $R^1 = H, R^2 = t\text{-Bu}: 78\%$ $R^1 = H, R^2 = Cy: 52\%$ $R^1 = OMe, R^2 = t\text{-Bu}: 80\%$
$CF_3CH_2SO_2Cl$	 $R^1 = H, R^2 = t\text{-Bu}: 81\%$ $R^1 = H, R^2 = Cy: 51\%$ $R^1 = OMe, R^2 = t\text{-Bu}: 85\%$

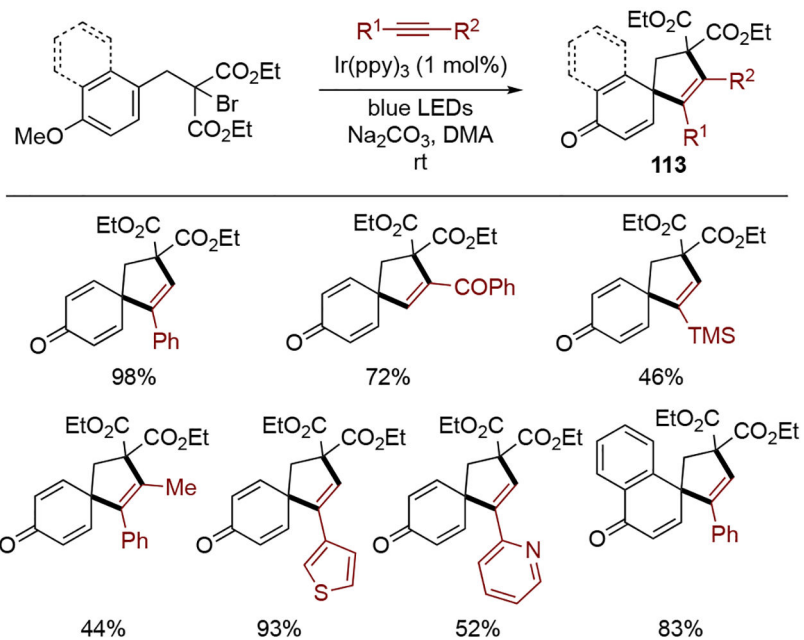
Scheme 31.Scope of dearomative spirocyclizations with *N*-(*p*-hydroxybenzyl)acrylamides.



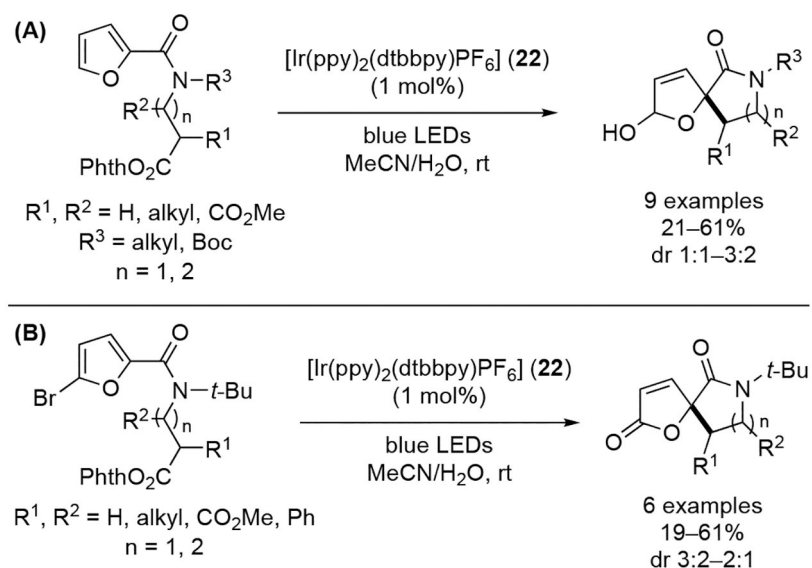
Scheme 32.
Proposed mechanism.

**Scheme 33.**

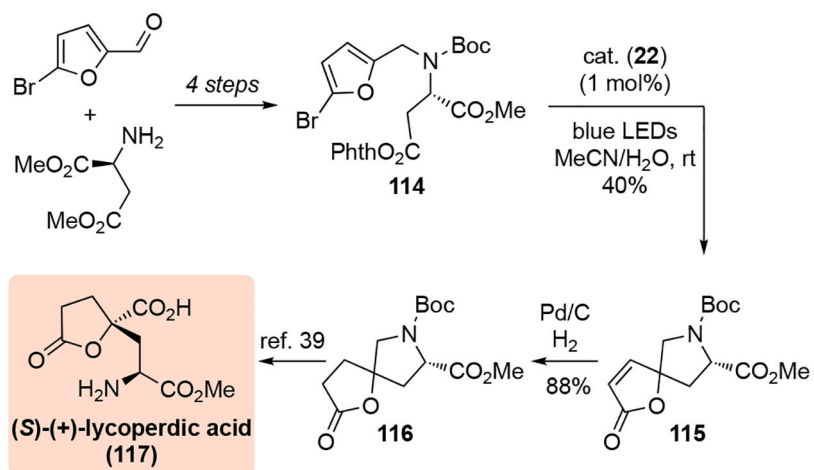
Synthesis of azaspiro[4.5]decane through dearomative radical cyclization.



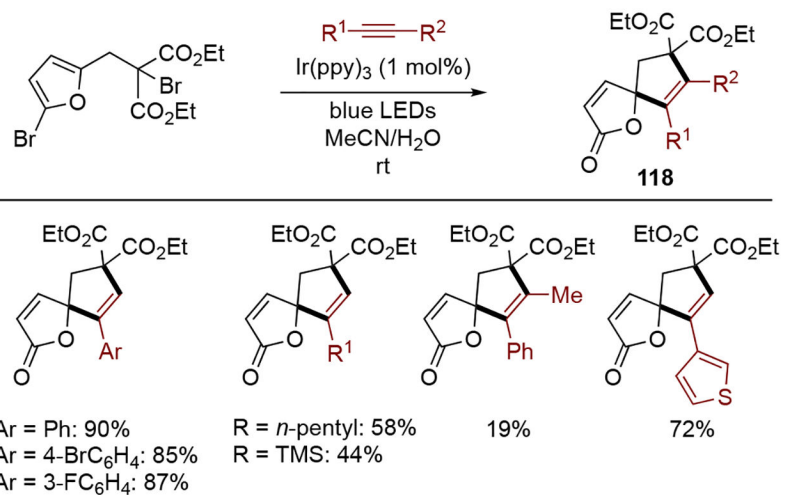
Scheme 34.
 Intermolecular dearomative radical cyclization.

**Scheme 35.**

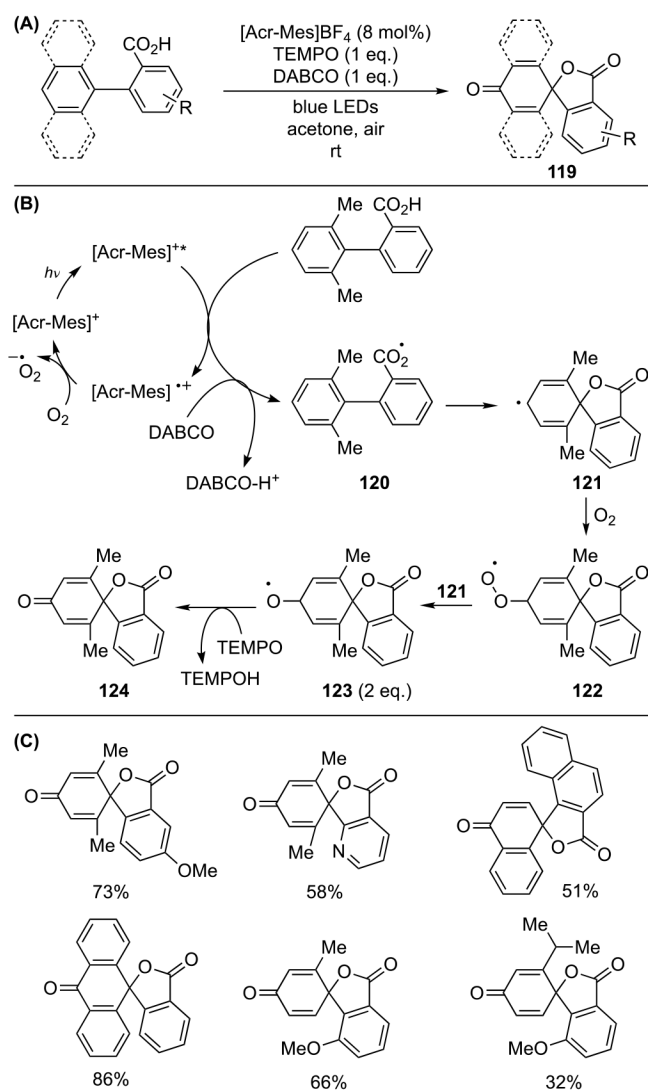
Visible-light-mediated synthesis of spirodihydrofuranols.



Scheme 36.
Synthesis of (*S*)-(+)-lycoperdic acid.

**Scheme 37.**

Intermolecular dearomative cyclization of 2-bromofurans.

**Scheme 38.**

Visible-light-mediated dearomative spiroactonization of biaryl compounds.